Research highlights

- Submicron superfine PAC (SSPAC, median diameter 200 nm) adsorbed biopolymer well.
- SSPAC removed biopolymer best due to straining effect and high adsorption capacity.
- Precoating SSPAC on a membrane reduced the rise of transmembrane pressure (TMP).
- Precoating SSPAC after coagulation prevented the rise of TMP almost completely.
- Pulse dosing for precoating prevented the rise of TMP better than continuous dosing.

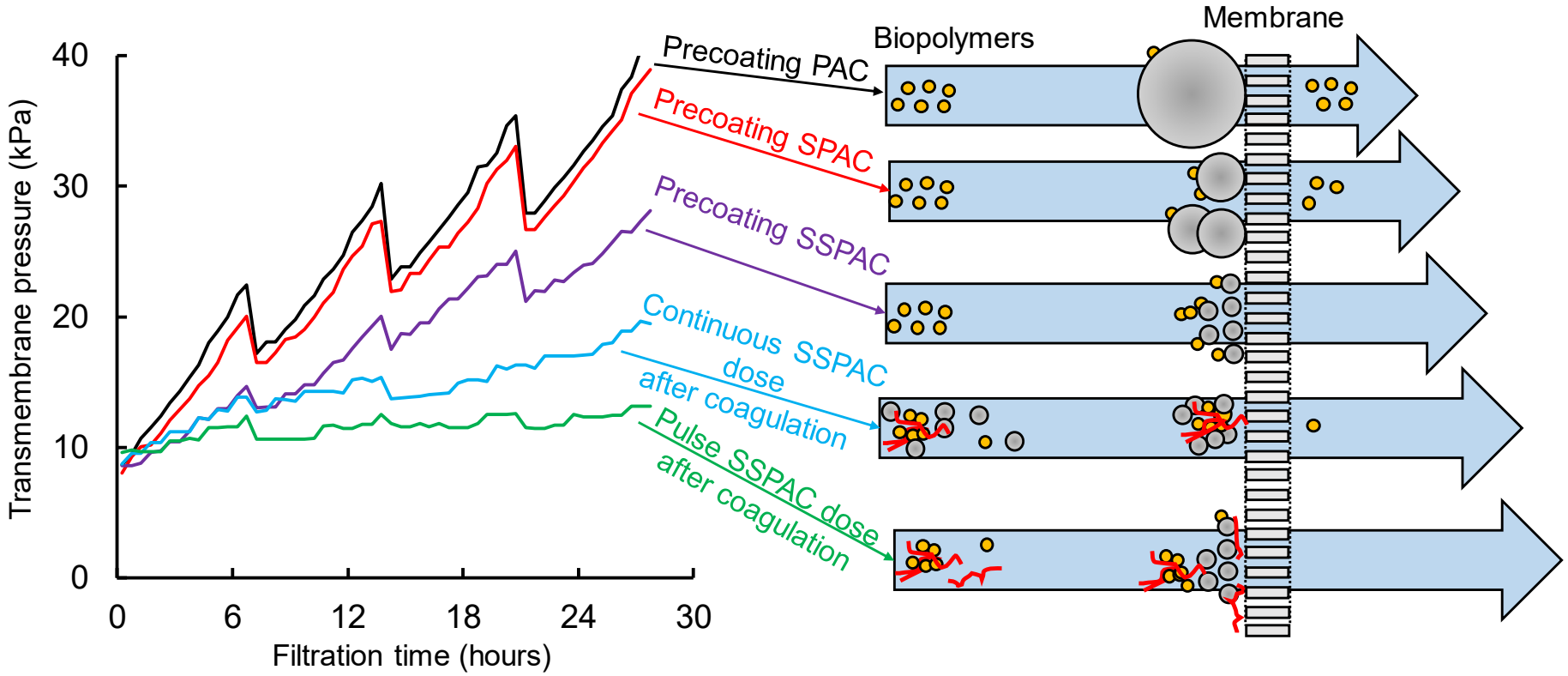
Transmembrane pressure (kPa)
40
30
20
10
0
0
6
12
18
24
30
Filtration time (hours)
Precoating PAC
Precoating SPAC
Precoating SSPAC
Continuous SSPAC dose after coagulation
Pulse SSPAC dose after coagulation
Biopolymers
Membrane

Precoating membranes with submicron super-fine powdered activated carbon after coagulation prevents transmembrane pressure rise: Straining and high adsorption capacity effects

Yuanjun Zhao [a], Ryosuke Kitajima [a], Nobutaka Shirasaki [b], Yoshihiko Matsui [b], Taku Matsushita [b]*

[a] *Graduate School of Engineering, Hokkaido University.*
N13W8 Sapporo 060-8628 Japan

[b] *Faculty of Engineering, Hokkaido University*
N13W8 Sapporo 060-8628 Japan

* *Corresponding author*. Tel./fax: +81-11-706-7280

E-mail address: matsui@eng.hokudai.ac.jp (Y. Matsui)

Abstract

Commercially available powdered activated carbon (PAC) with a median diameter of 12–42 μm was ground into 1 μm sized superfine PAC (SPAC) and 200 nm sized submicron SPAC (SSPAC) and investigated as a pretreatment material for the prevention of hydraulically irreversible membrane fouling during a submerged microfiltration (MF) process. Compared with PAC and SPAC, SSPAC has a high capacity for selective biopolymer adsorption, which is a characteristic found in natural organic matter and is commonly considered to be a major contributor to membrane fouling. Precoating the membrane surface with SSPAC during batch filtration further removes the biopolymers by straining them out. In lab-scale membrane filtration experiments, an increase in the transmembrane pressure (TMP) was almost completely prevented through a precoating with SSPAC based on its pulse dose after coagulation pretreatment. The precoated SSPAC formed a dense layer on the membrane preventing biopolymers from attaching to the membrane. Coagulation pretreatment enabled the precoated activated carbon to be rinsed off during hydraulic backwashing. The functionality of the membrane was thereby retained for a long-term operation. Precoating the membranes with SSPAC after coagulation is a promising way to control membrane fouling, and efficiently prevents an increase in the TMP because of the straining effect of the SSPAC and the high capacity of the SSPAC to adsorb any existing biopolymers.

Keywords:

SSPAC

SPAC

Membrane fouling

TMP

Filtration

1. Introduction

Although low-pressure membrane technology (e.g., microfiltration and ultrafiltration) is used worldwide in drinking water treatments, the practical application of this technology is constrained through membrane fouling (Filloux et al., 2016, 2012; Luo et al., 2018; Yu et al., 2018). An increase in the transmembrane pressure (TMP) caused by membrane fouling, particularly hydraulically irreversible membrane fouling, leads to high rates of energy consumption and a long-term degradation of the system performance.

Natural organic matter (NOM) is present in all bodies of water and plays an important role in membrane fouling. The chemical structure of NOM, however, is not well understood because its composition is variable and the chemical constituents that make up NOM have a wide range of molecular weights (Adusei-Gyamfi et al., 2019; Amy, 2008; Lee et al., 2004). The introduction of liquid chromatography-organic carbon detection (LC-OCD) used to separate NOM into various fractions (Huber et al., 2011) has revealed that a hydrophilic fraction that includes compounds with high molecular weights (also known as biopolymers) is the main cause of hydraulically irreversible membrane fouling (Ayache et al., 2013; Chen et al., 2016; Huang et al., 2017; Kimura et al., 2014; Tian et al., 2013; Wang and Li, 2008; Zheng et al., 2010).

Activated carbon (AC) adsorption, coagulation, and other pretreatment methods have been widely investigated to remove NOM (particularly biopolymers) prior to membrane filtration and to thus retard the long-term buildup of TMP (Cheng et al., 2017; Ding et al., 2018; Fabris et al., 2007; Jarvis et al., 2012; Kimura and Oki, 2017; Lee et al., 2006; Ma et al., 2014; Su et al., 2017; Umar et al., 2016; Wang et al., 2013; Xing et al., 2019). AC adsorption, coagulation,

and the combination of both have been studied for NOM removal in pilot plants (Keeley et al., 2016; Kweon et al., 2009; Wang et al., 2014). Although pretreatment using only powdered activated carbon (PAC) in an ultrafiltration system has produced a high removal of NOM, the PAC itself has caused severe membrane fouling (Lin et al., 2001, 1999). Recent studies, however, have produced more satisfactory results; when PAC is dosed at the very beginning of the filtration or is pre-deposited (referred to as a precoating) on the surface of the membrane, membrane fouling is prevented to a certain extent (Campinas, 2010; Kim et al., 2008; Ye et al., 2006). The reasons for these inconsistent results may be the hydrophobicity of the membrane and the diverse characteristics of raw waters. PAC causes less fouling with hydrophilic membranes (Crozes et al., 1993), and helps reduce fouling when its use is combined with coagulation pretreatment, although such a combination does not completely eliminate fouling. As a result, TMP increases gradually during long-term operation (Kweon et al., 2009).

Furthermore, superfine PAC (SPAC, median diameter of ~1 μm), which is produced through the milling of ordinary PAC, has been found to more rapidly adsorb NOM than PAC and to have a higher NOM adsorption capacity; in addition, the required dosages are smaller (Amaral et al., 2016; Bonvin et al., 2016; Matsui et al., 2007, 2006, 2005, 2004). Dosing with SPAC as a membrane pretreatment method in combination with coagulation has resulted in high rates of NOM removal and the ability to mitigate the buildup of TMP (Matsui et al., 2009). Although biopolymers are efficiently removed through a precoating with SPAC, the SPAC layer itself reduces the permeability of the membrane (Heijman et al., 2009). However, the efficacy of the SPAC precoating combined with coagulation pretreatment remains unexplored. Recent studies on submicron SPAC (SSPAC) with a median diameter of ~200 nm have revealed that when the size of the PAC decreases from 30 μm to 140 nm, its capacity to adsorb NOM increases over the entire range of SSPAC particle sizes (Pan et al., 2017).

To determine the biopolymer adsorption capacity of SSPAC, we conducted adsorption

isotherm experiments using PAC/SPAC/SSPAC and biopolymers in natural river water. Furthermore, we conducted batch-scale submerged membrane filtration experiments to elucidate the mechanism of the biopolymer removal. Laboratory-scale membrane filtration experiments with treatments combining PAC/SPAC/SSPAC and coagulation under different dosing regimes were further investigated to compare the ability of the treatments to prevent a long-term increase in TMP during filtration with periodic backwashes.

2. Materials and methods

2.1. ACs

In this study, we used wood-based PAC (Taiko-W, Futamura Chemical Co., Ltd., Nagoya, Japan), SPAC, and SSPAC. A PAC slurry was made by dosing PAC into pure water (Milli-Q water, Merck KGaA, Darmstadt, Germany). The PAC concentration was consistently within the range of 10–15% (w/w). The PAC slurry was then milled in a closed chamber with alumina balls (diameters of 5 and 10 mm) at 45 rpm for 5 h to obtain AC with a median diameter (D50) of ~4 μm. The milled slurry was then further milled using a bead mill (LMZ015, Ashizawa Finetech, Ltd., Chiba, Japan) with zirconium dioxide beads (diameter of 0.3 mm) in recirculation mode at 2,590 rpm for 30 min to produce SPAC with a D50 of ~1 μm. SSPAC was produced from the same AC slurry using a bead (diameter of 0.1 mm) mill at 3,884 rpm for 2 h to achieve a D50 of ~200 nm.

We measured the size distribution of the AC particles using a laser-light-scattering instrument (Microtrac MT3300EXII, Nikkiso Co., Inc., Tokyo, Japan). A dispersant (Triton X-100, Kanto Chemical Co., Inc., Tokyo, Japan) was dosed into the samples, which were then sonicated (150 W, 19.5 kHz) for approximately 1 min in the case of PAC/SPAC and for 6 min

for SSPAC to break up the particle aggregates and determine the true particle sizes (Pan et al., 2016). The particle size distributions of the ACs are shown in Fig. 1S of the supplementary information (SI).

2.2. Water

The water of the Wanigawa River (Ibaraki, Japan) was sampled in May and November of 2017. The samples were shipped to the authors' laboratory and designated as raw water-1 and raw water-2, respectively. The water qualities of the two waters were not significantly different (Table 1S, SI). The samples were then filtered through mixed cellulose ester (MCE) membrane filters with a pore size of 0.1 μm (ϕ142 mm, Merck KGaA, Darmstadt, Germany) to obtain a working solution for the adsorption isotherm experiments (Section 2.3) and batch precoat filtration experiments (Sections 2.4 and 2.5). A coated cellulose acetate membrane filter with a pore size of 10 μm (ϕ142 mm, Toyo Roshi Kaisha, Ltd., Tokyo, Japan) was used to produce 7 L of raw water for the experiments involving the AC addition and submerged membrane filtration with a backwash (Section 2.6). Ultraviolet absorbance at 260 nm (UV260) and the concentrations of biopolymer, humic substances, and total organic carbon (TOC) were used as metrics of the concentrations. TOC concentration was determined using a TOC analyzer (Model 900, Sievers Instruments, Boulder, CO, USA). In addition, the UV260 was analyzed using a UV spectrophotometer (UV-1800 with a 5 cm cell, Shimadzu, Kyoto, Japan). The biopolymer and HS concentrations were analyzed using an HPLC system (1100 series, Agilent Tech, Tokyo, Japan) consisting of a single column (Toyopearl HW-50S, 250 mm × 20 mm, Tosoh Inc., Tokyo, Japan), an injection system (injection rate of 1.2 mL/min), a UV detector, and a TOC analyzer (M9e, Central Kagaku Corp., Tokyo, Japan). The use of this system to measure the biopolymer

and HS concentrations corresponds to the application of the size-exclusion chromatography method developed by Huber et al. (2011).

2.3. Adsorption isotherm experiments

The PAC/SPAC/SSPAC particles were injected into shaking flasks containing 100 mL of raw water-2 at fixed carbon dosages of 0, 5, 10, 20, 30, and 40 mg/L. The sealed flasks were then shaken at room temperature (20 °C) for 1 week. The water in the flasks was taken out and then centrifuged. The supernatant was filtered through two stacked membrane filters, namely, polyvinylidene fluoride (PVDF), with a pore size of 0.2 μm (Dismic-25CS, Advantec Toyo Kaisha, Ltd., Tokyo, Japan) to remove residual AC that may interfere with further water quality analyses.

2.4. Batch precoat single filtration

The PAC, SPAC, and SSPAC particles and two sizes of polystyrene latex spheres (D50 values of 100 and 200 nm, henceforth referred to as PSL100 and PSL200, Micromod Partikeltechnologie GmbH, Rostock, Germany) were separately dosed into 50 mL of raw water-1. Each suspension was poured into a membrane filter funnel with a flat sheet MCE membrane (pore size of 0.1 μm, ϕ47 mm, and an effective membrane filtration area of 9.6 cm^2, Merck KGaA). Next, 40 mL of the suspension was then filtered through the membrane by a vacuum (−80 kPa) to obtain an initial AC deposition mass of 0.17, 0.35, or 0.53 mg/cm^2 on the surface of the membrane. Ten milliliters of the suspension remained in the funnel. Another 50 mL of raw water-1 was then poured carefully into the funnel without breaking the precoating, and the filtration was resumed. The filtration was continued until 50 mL of the filtrate was collected for

168 the biopolymer analysis. The increase in the AC deposition mass during the 50-mL filtration
169 was small (10%).
170
171 *2.5. Batch precoat repeat filtration*
172
173 Fifty milliliters of raw water-1 containing 84 mg/L of an AC suspension was poured into a
174 membrane filter funnel, and 40 mL was filtered through the membrane to form an AC
175 precoating. Then, 50 mL of raw water-1 was added to the funnel and allowed to pass through
176 the filter. This process (the addition of 50 mL of raw water-1 + filtration) was repeated until the
177 total filtrate volume reached 2,090 mL per filter. The filtrates were then sampled to determine
178 the biopolymer concentrations. In some of the experiments, an AC precoating was applied after
179 the AC suspension was sonicated (150 W, 19.5 kHz) for 3 min.
180
181 *2.6. AC addition and submerged membrane filtration with backwash*
182
183 Fig. 1 shows a schematic diagram of the experimental setup. Raw water-2 was fed by means of
184 a peristaltic pump with a constant flow rate of 0.64 mL/min into a rectangular tank (interior
185 dimensions of 1.1 cm × 1.1 cm, water depth of 27.5 cm) in which a hollow fiber PVDF
186 membrane fiber with a pore size of 0.1 μm (Asahi Kasei Corp., Tokyo, Japan) with its tip closed
187 was submerged (the PVDF fiber had been purchased as a membrane module and cut to a length
188 of 14 cm with an effective filtration area of 6 cm^2). Prior to use in the experiments, every fiber
189 was tested to ensure that the TMP was within the range of 46–48 kPa during filtration of Milli-
190 Q water at a flow rate of 15 m/day (625 L/m^2 h). Filtration at a flow rate of 1.7 m/day (70.8
191 L/m^2 h) was achieved by applying a vacuum to the inside of the membrane. The filtration lasted
192 for 28 h with a periodic hydraulic backwash. The hydraulic backwash was conducted at 7 h

intervals by introducing pure water at 50 kPa from the filtrate side, and the suspension in the tank was then drained. Membrane filtrate was collected at 30 min intervals for analysis.

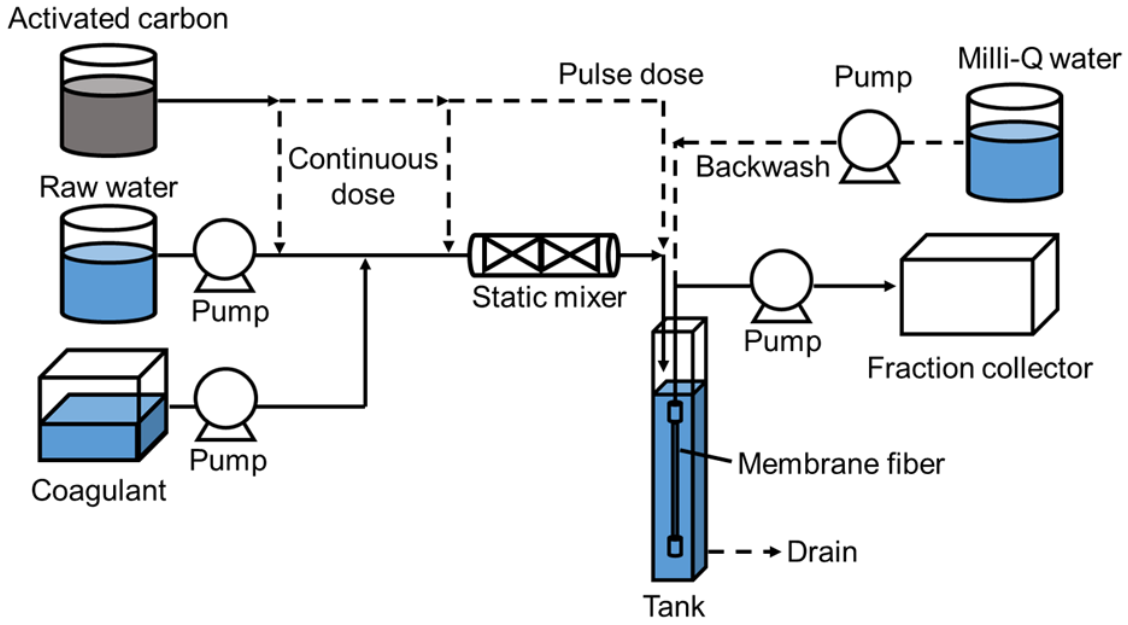

Fig. 1 — Laboratory setup for additions of activated carbon and coagulant and for submerged membrane filtration with backwash.

AC was added to the system in a pulse dose prior to the start of the filtration (referred to as Methods A, B, and C in Figs. 2S–4S, SI) after hydraulic backwash or added through a continuous dose (referred to as Methods D and E in Figs. 5S and 6S, SI) throughout the entire filtration process. In the pulse AC dose experiments, two methods of AC injection were used (Fig. 7S, SI). In the direct pulse dose methods (Methods A and B), AC was injected directly into the membrane tank followed by 3 min of bubbling with air at 3.2–5.2 L/min from the bottom of the tank. In the indirect pulse dose method (Method C), AC and raw water were mixed vigorously in a bottle, and the mixture was then injected into the membrane tank. In all experiments, AC dosages were fixed at 5 mg-C/L. The dosage in the case of a pulse dose was

expressed as the average dosage, which was equated to the mass of AC (milligram) divided by the volume (liter) of treated raw water.

In Methods B–E (Figs. 3S–6S, SI), a static mixer was placed in the feed line to the tank. Polyaluminum chloride coagulant (basicity 2.1; sulfate ion 2% (w/w), Taki Chemical Co., Hyogo, Japan) was injected at 2 mg-Al/L and mixed with a static mixer. In Methods B and C (pulse AC dose), coagulant injection and mixing were applied before the AC dose (Figs. 3S and 4S, SI). In Methods D and E (continuous AC dose), coagulant injection and mixing were conducted either before or after the AC dose (Figs. 5S and 6S, SI).

Raw water was supplemented with HCl or NaOH such that the filtrate pH became roughly constant at 7.5. The suction pressure was recorded based on the voltage using a digital pressure meter (GC61, Nagano Keiki Products, Tokyo, Japan) and converted into pressure using calibration curves determined during each experiment. The experiment was conducted in a room with a temperature of ~25 °C. During the experiment, the water temperature was measured using a digital thermometer (LR5011, Hioki E.E. Corp., Nagano, Japan), and TMP was normalized to 25 °C to avoid the influence of changes in the viscosity.

3. Results and discussion

3.1. Biopolymer and TOC adsorption capacities

Adsorption isotherms of biopolymer, TOC, and UV260 were obtained on SSPAC, SPAC, and PAC (Fig. 8S–10S, SI). The adsorption capacities of the three ACs for biopolymer, TOC, and UV260 increased in order of PAC < SPAC < SSPAC. This order corresponds to the descending order of the AC particle size. The fact that the adsorption capacities were enhanced as the

particle size of the AC decreased is in accordance with the recent discovery that the adsorption capacity of AC toward adsorbates with a high molecular weight increases as the particle size of the AC decreases (D50 from 30 μm to 140 nm) (Pan et al., 2017). This is because the molecules are mostly adsorbed on the exterior of the particles (Ando et al., 2011; Matsui et al., 2014, 2013, 2011). The change in the AC particle size caused by the milling does not result in any substantial change in the internal pore area (Pan et al., 2017).

To further clarify the dependence of the adsorption capacity on the AC particle size, we plotted the solid-phase concentration at equilibrium with a liquid-phase concentration of 1.8 mg/L (TOC) and 0.02 mg/L (biopolymer) against the D50 of the AC particles (Fig. 2). The adsorption capacity of the AC for the biopolymer was smaller than that for the TOC because biopolymers are constituents of NOM, and the biopolymer concentrations are therefore lower than the NOM concentrations (which are determined from the TOC). As the D50s of the ACs decreased, their capacities to adsorb both biopolymers and TOC increased. However, the adsorption capacity for the biopolymer depended more strongly on the AC particle size than did the adsorption capacity for the TOC. These trends held when the data were plotted for different equilibrium liquid-phase concentrations (Fig. 11S, SI). Of relevance to the capacity dependency on the AC particle size is the adsorption of high molecular-weight compounds mainly on the exterior of the AC particles owing to their limited intraparticle diffusion distances (Ando et al., 2011; Matsui et al., 2011). Ando et al. (2010) reported that the capacity dependency is large for large molecules. In our study, therefore, the strong dependence of the biopolymer adsorption capacity on the AC particle size was likely related to the large molecular size of the biopolymers in the NOM. Because of the different degrees of capacity dependency between the biopolymer and NOM, the biopolymer/TOC concentration ratio after AC contact decreased with the SSPAC and SPAC dosages, but increased with the PAC dosage (Fig. 12S, SI). Moreover, the biopolymer/TOC concentration ratio decreased more rapidly after the

SSPAC contact than after the SPAC contact. These results indicate that SSPAC selectively adsorbs the biopolymer from the NOM compared with SPAC and PAC.

Because biopolymers are commonly considered to be a major membrane foulant (Huber et al., 2011; Kimura et al., 2014; Myat et al., 2014; Tian et al., 2013; Zheng et al., 2010), these results suggest that adsorption pretreatment by SSPAC will mitigate the membrane fouling and attenuate the TMP buildup more efficiently than SPAC and PAC pretreatment. Heijman et al. (2009) have a higher biopolymer removal by SPAC than by PAC and suggest that if SPAC is evenly loaded on a membrane, it will remove the biopolymers and thereby decrease the membrane fouling. However, SSPAC is clearly superior to the SPAC.

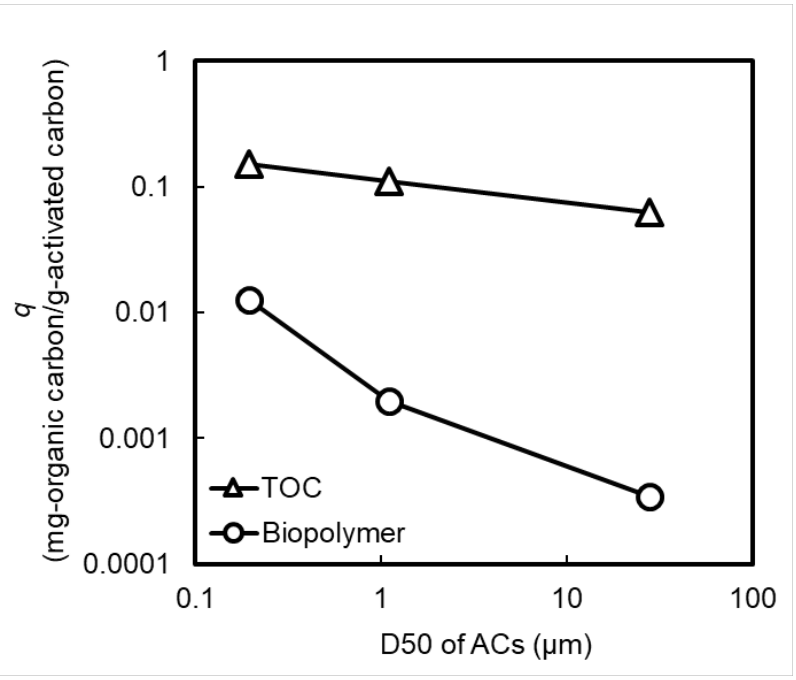

Fig. 2 — Plots of solid-phase concentration (*q*) at an equilibrium liquid-phase total organic carbon (TOC) concentration of 1.8 mg/L and a biopolymer concentration of 0.02 mg/L versus the median diameter (D50) of the activated carbons (ACs). The data are taken from Figs. 8S and 9S, SI. Raw water-2 was used in this experiment.

3.2. Biopolymer removal by batch precoat single filtration

Fig. 3 shows the results of precoat experiments during which PAC, SPAC, SSPAC, PSL100, and PSL200 particles were each deposited on a 0.1 μm MCE flat sheet membrane filter to produce a precoat layer, and a sample water containing biopolymers was then passed through the membrane with a precoating. As described in Section 2.4, the raw water in the experiments was filtered through a 0.1-μm MCE membrane filter. Therefore, biopolymers were not removed simply by the water passing through the 0.1-μm MCE membrane filters used for the precoating (Fig. 13S, SI). The fact that the biopolymers were not removed by the membrane filtration alone (Fig. 13S, SI) make it clear that the biopolymer removal was possible only when the membrane was precoated with polystyrene latex particles or AC particles.

The biopolymer removal rates increased as the amount of particles precoating the membrane increased. However, the removal by the PSL-precoated membrane reached a plateau after a certain amount of PSL precoating. The plateau of the biopolymer removal rate was higher for the PSL100 particles than for the PSL200 particles. Biopolymer removal by the SPAC/SSPAC-precoated membranes was high and can be attributed to the adsorption of biopolymers onto the AC. However, the removal by a PSL precoating cannot be attributed to adsorption because no adsorption occurred (Fig. 14S, SI). Biopolymer removal from the PSL100 particles may have been due to a straining effect. If the ratio of particle diameter to media diameter is greater than 0.15, the particle will be stained by the media (Crittenden et al., 2012). Therefore, the PSL100 (100 nm) media could strain particles with the size > 15 nm. On the other hand, biopolymer of extremely large molecular weights (> 1 million Da) has high fouling potentials for MF (Kimura et al., 2018), and such molecular weights could be converted to molecular diameters > 17 nm (Weiss et al., 2018). The estimation of the molecular diameters > 17 nm is in accordance with the particle size distribution of the biopolymer determined by membrane filtration (Fig. 15S,

SI). Therefore, most of the biopolymer molecules would be greater than 15 nm in size. The biopolymer molecules are too large to pass through the interstitial spaces between the PSL particles and are captured as the flow of water moves them through the particles The higher rate of biopolymer removal by the precoating of PSL100 versus the PSL200 particles is in accordance with this postulated straining mechanism. The difference in removal rates can be explained if there is variability in the sizes of the biopolymer molecules (Kimura et al., 2018). The interstitial spaces are smaller in a precoating by PSL100 particles versus that by PSL200 particles, and the former can therefore filter the biopolymer molecules over a wider range of molecular sizes, including relatively small molecules. The fact that the straining effect can remove biopolymer molecules larger than a certain size but cannot filter biopolymers smaller than this size explains why the biopolymer removal plateaued as the amount of PSL precoating increased. The abilities of PAC, SPAC, and SSPAC to remove biopolymers were also consistent with the particle sizes of the ACs: SSPAC achieved the highest removal, followed by SPAC and then PAC. This result reflects the higher adsorption capacity as well as the higher straining effect of SSPAC.

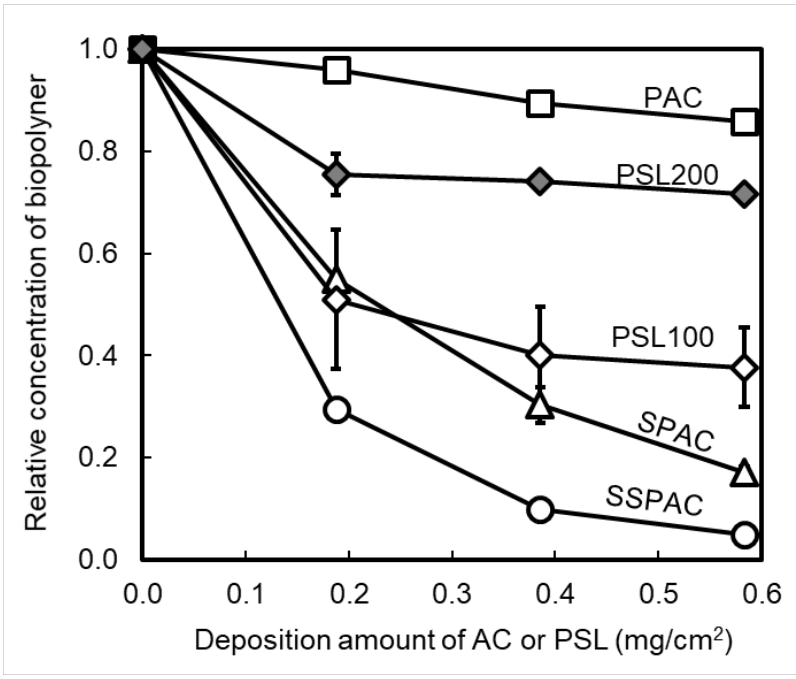

Fig. 3 — Fractions of biopolymers that remained after passing through a precoated membrane versus amounts of activated carbon (AC) or polystyrene latex spheres (PSLs) precoating the membrane. Biopolymer concentration was determined for 50-mL filtrate samples taken after precoating by filtering a 40-mL sample. Error bars indicate ranges of two measurements by liquid chromatography-organic carbon detection methodology. Raw water-1 was used in this experiment.

3.3. Biopolymer removal by batch precoat repeated filtration

We conducted batch precoat repeated filtration experiments to further clarify the straining effect of SPAC and SSPAC particles on the biopolymer removal. Fig. 4 shows the percentage of biopolymers remaining in the filtrates versus the filtration volume per membrane surface area. The fact that the biopolymer concentration in the filtrate was low at the beginning of the filtration (i.e., the biopolymer removal was high) was probably due to the fact that the AC was fresh and had a high adsorption capacity. The biopolymer concentration in the filtrate increased as the filtration progressed but did not reach the influent concentration level. The biopolymer concentration plateaued at a level of less than the inflow concentration. This result indicates that there was a certain degree of removal maintained by the straining effect even after the adsorption capacity had been fully saturated. This stable level of removal was higher with the

SSPAC precoating than with the SPAC precoating, and was higher when AC particles were sonicated before precoating than when they were not (compare the white and gray symbols in Fig. 4). SSPAC and SPAC particles mildly agglomerate when produced by milling (Pan et al., 2016). AC particles sufficiently dispersed by sonication can therefore deposit densely on a membrane and thereby strengthen the straining effect.

A biopolymer is known to be a membrane-fouling substance. The high biopolymer removal by SSPAC owing to its high adsorption capacity and straining effect strongly suggests that precoating a membrane with SSPAC can mitigate the increase in TMP during the operation of a membrane filtration system.

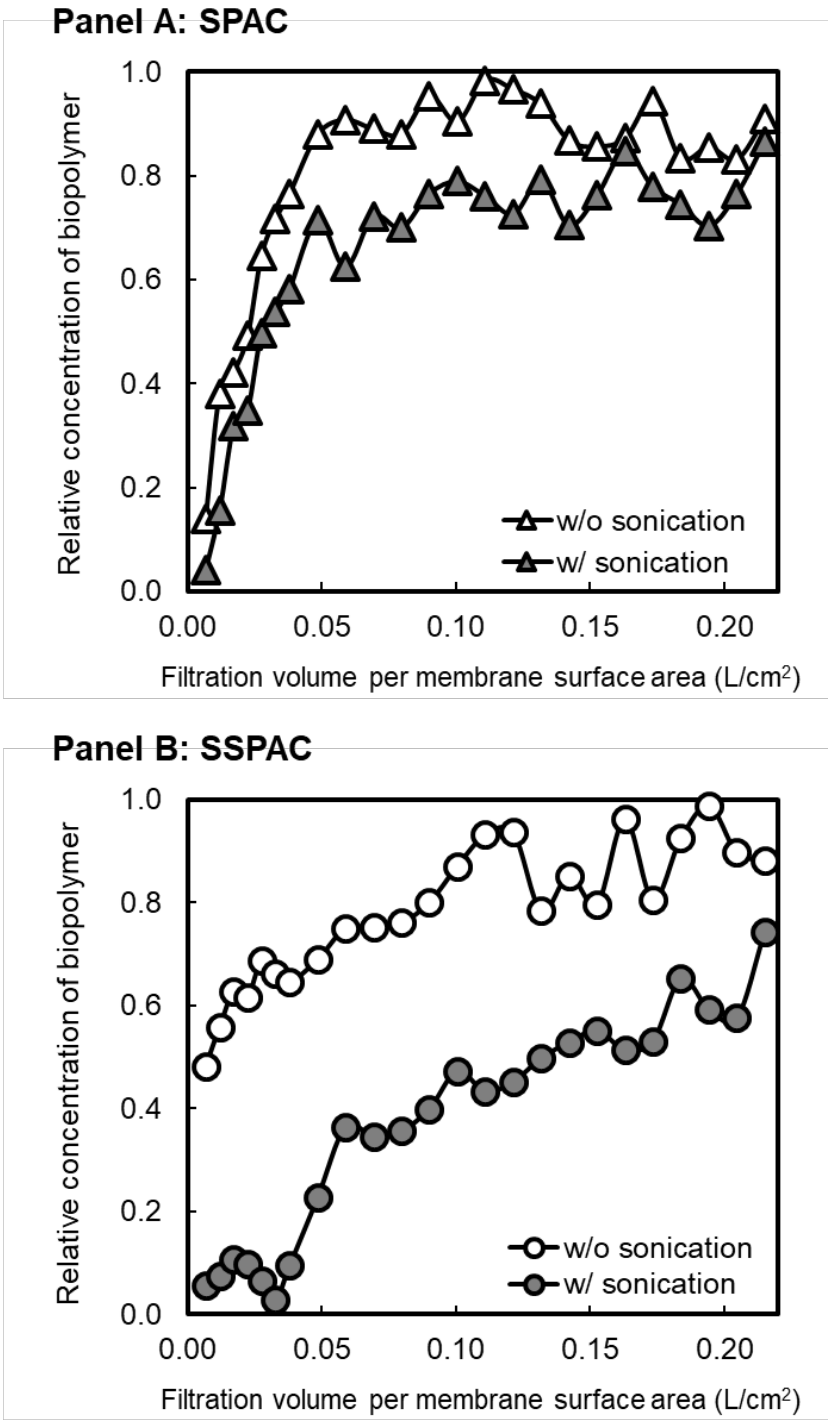

Fig. 4 — Relative concentration of biopolymer versus filtration volume per membrane surface area of water samples. The amount of powdered activated carbon (PAC) deposited on the membrane for precoating was 0.38 mg/cm^2. Panel A: SPAC. Panel B: SSPAC. Raw water-1 was used in this experiment.

3.4. Changes in TMP during AC addition and membrane filtration with backwash

Fig. 5 shows the changes in the TMP during filtration with periodic backwashes. During the experiments (Method A), AC was dosed just after every backwash using a direct pulse dose to make a precoat on the membrane. Among the three ACs, SSPAC alleviated the increase in the TMP the most, followed by SPAC and PAC. TMP increased rapidly without an AC pretreatment. However, even with SSPAC pretreatment, TMP increased with time. Hydraulic backwashes, which were conducted every 7 h, canceled the increase in the TMP to only a certain extent. The implication here is that hydraulically irreversible membrane fouling cannot be stopped simply by precoating with SSPAC.

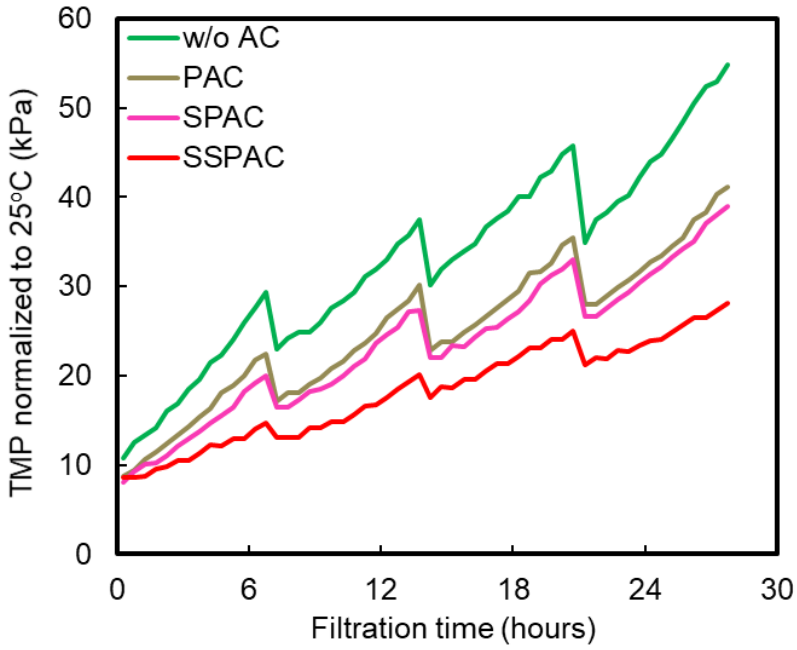

Fig. 5 — TMP versus filtration time for powdered activated carbon (PAC), superfine PAC (SPAC), and submicron SPAC (SSPAC). The experiments were conducted by Method A, where direct pulse dosing (explained in Figs. 2S and 7S, SI) was used. Backwash interval was 7 hours. Filtration rate was 1.7 m/day (70.8 L/m^{2}h). Raw water-2 was used in this experiment.

382 The addition of SPAC during membrane filtration is already being used in full-scale water
383 treatments (Kanaya et al., 2015). SPAC has not been added intermittently to form a precoating,
384 but instead has been added continuously prior to coagulation pretreatment. A continuous SPAC
385 addition followed by coagulation pretreatment has successfully mitigated an increase in the
386 TMP better than coagulation pretreatment alone, and the efficacy of adding SPAC followed by
387 coagulation pretreatment (Matsui et al., 2009) implies the important role of coagulation in
388 controlling the membrane fouling. We therefore conducted experiments using both coagulation
389 and AC pretreatment. Fig. 6 shows a comparison of the changes in the TMP in systems with
390 and without coagulation pretreatment. The fact that TMP increases at a much lower rate with
391 coagulation than without coagulation indicates that coagulation pretreatment before AC dosing
392 is necessary to mitigate membrane fouling.
393

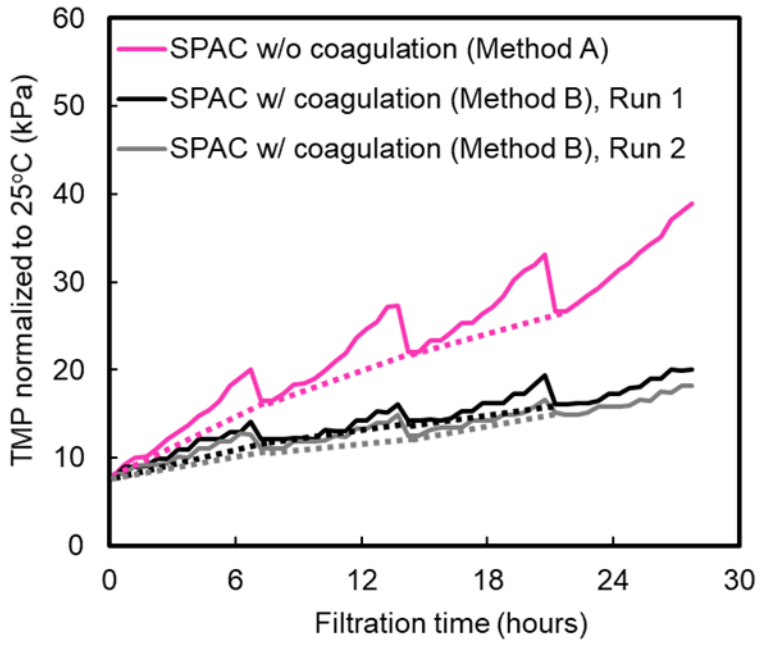

394

395 **Fig. 6 — TMP versus filtration time with/without coagulation. The experiments were conducted**
396 **by Methods A and B, where direct pulse dosing (explained in Figs. 2S, 3S and 7S, SI) of superfine**
397 **powdered activated carbon (SPAC) was used. Dotted lines show TMP rise due to hydraulically**
398 **irreversible fouling. Backwash interval was 7 hours. Filtration rate was 1.7 m/day (70.8 L/m^2 h).**
399 **Raw water-2 was used in this experiment.**
400

401

It is widely known that coagulation can remove biopolymers to a certain extent and mitigate an increase in the TMP (Jung et al., 2006; Kimura et al., 2018; Wray and Andrews, 2014). During coagulation treatment, NOMs (including biopolymers) are coagulated to form large flocs. This process increases the permeability of the gel cake layer formed on the membrane surface and thereby mitigates an increase in the TMP. Experiments with and without coagulation pretreatment (Fig. 6) were conducted using the same water and the same AC dose. The depositions on the membrane will therefore be similar, although the fact that the rate of increase in the TMP during each filtration cycle was lower with coagulation than without coagulation suggests that the material deposited on the filters was more permeable in the former case.

Membrane fouling, which causes an increase in the TMP, is divided into hydraulically reversible and irreversible fouling. On the one hand, hydraulically reversible fouling can be physically removed (e.g., using a backwash). On the other hand, hydraulically irreversible fouling can be removed only through chemical cleaning methods, which require more time and effort than a backwash (Kimura et al., 2008; Peiris et al., 2013). The control of hydraulically irreversible fouling is therefore extremely important for a reduction in the operational cost during the membrane filtration process. The dotted lines in Fig. 6 show the changes in the increase in TMP through hydraulically irreversible fouling. SPAC dosing through direct pulses mitigates irreversible fouling better with coagulation pretreatment than without such a pretreatment. Fig. 7 shows photographs of a membrane-submerged tank during a hydraulic backwash (Fig. 16S shows similar results in the case of SSPAC). The membrane remained black because of AC accumulation in the system without coagulation pretreatment, whereas the membrane became white because of a detachment of the floc particles during a backwash in the system with coagulation pretreatment. A more severe hydraulically irreversible fouling that occurs without coagulation pretreatment may therefore be due to the attachment of AC particles

on the membrane along with the NOM, including biopolymers. Coagulation alleviates the attachment of AC particles on the membrane. Hydrolysis of the aluminum polymer formed from the polyaluminum chloride coagulant will impede the strong attachment of AC to the membrane and can thereby facilitate the release of the AC attached to the membrane during a backwash.

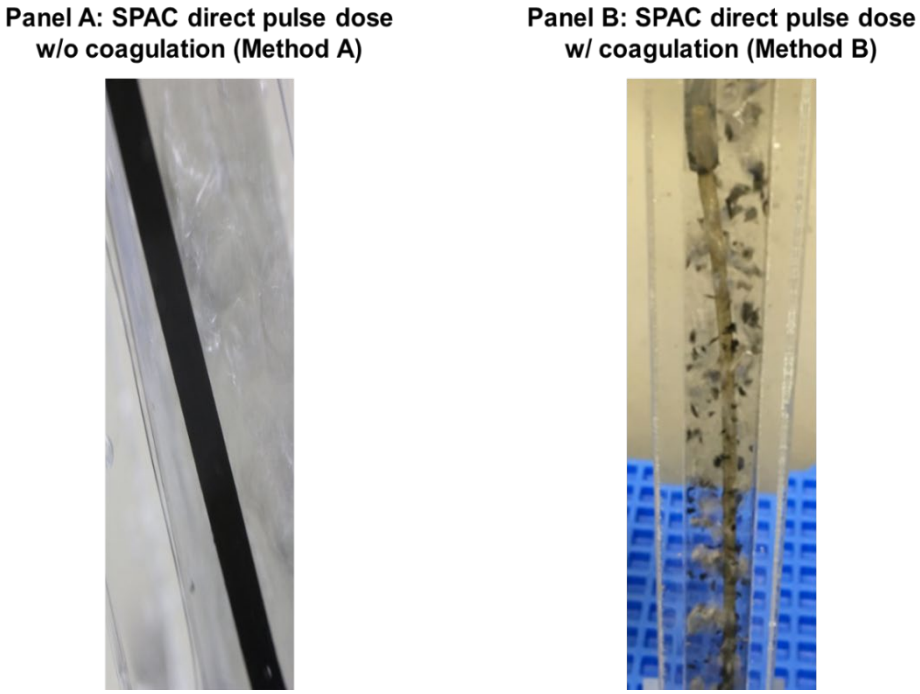

Fig. 7 — Photographs of a membrane tank during backwash. Panel A is a picture of the system without coagulation pretreatment (Method A). Panel B is a picture of the system with coagulation pretreatment (Method B). Direct pulse dosing (explained in Figs. 2S, 3S, and 7S, SI) was used in the experiments. Backwash pressure was 50 kPa. Filtration rate was 1.7 m/day (70.8 L/m^2 h). Raw water-2 was used in this experiment.

Membrane filtration experiments with continuous and pulse AC dosing were conducted to compare the effectiveness of a precoating as a means of controlling the membrane fouling. In the pulse AC dose experiments, AC was dosed only after the hydraulic backwash was applied to re-form the precoating. Two methods were used to continuously apply an AC dose. The

446 method for dosing the AC before coagulation (Method D) was taken from the methodology in
447 use at full-scale water treatment plants (Kanaya et al., 2015); to facilitate a comparison with the
448 pulse AC results, the method for dosing the AC continuously after coagulation (Method E) was
449 identical to that used in the pulse dose experiments (Method B) in terms of the sequence applied.
450 Figs. 17S (SI) and Fig. 8 compare the changes in TMP between the systems with continuous
451 AC dosing (Methods D and E) and pulse AC dosing (Method B, for precoating) for SPAC (Fig.
452 17S) and SSPAC (Fig. 8). For SSPAC, the TMPs increase at slower rates in both the direct and
453 the indirect pulse dose experiments than in the continuous dose experiments. The superiority of
454 the pulse dose to the continuous dose methodology for preventing an increase in the TMP was
455 confirmed during the experiments in which SSPAC was added as a pulse or continuously after
456 coagulation treatment. The amount of SSPAC used to precoat the membrane was higher for the
457 pulse dose method than for the continuous dose method from the beginning of the filtration.
458 The precoating prevented biopolymers from attaching to the membrane through the adsorptive
459 removal of the biopolymers and based on the straining effect described in Sections 3.1 and 3.2.
460 The superiority of the pulse dose method over continuous dosing for precoating was clear for
461 SSPAC (Fig. 8), but was less apparent for SPAC (Fig. 17S, SI). Precoating using AC to mitigate
462 membrane fouling was therefore effective when the AC particles were within the submicron
463 range. In other words, continuous dosing, which is simpler than pulse dosing, is a reasonable
464 dosing method if the AC particles are within the micron range.
465

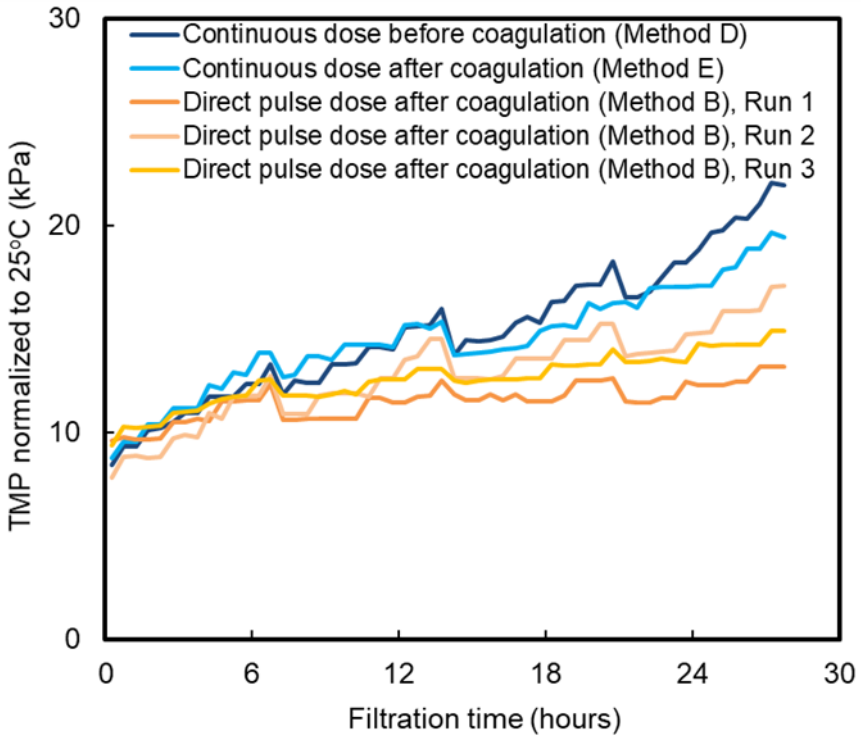

Fig. 8 —TMP as a function of filtration time when membrane filtration was conducted after SSPAC adsorption and coagulation pretreatment. The experiments were conducted by Methods B, D, and E (explained in Figs. 3S, 5S, and 6S, respectively, SI) to compare direct pulse dose and continues dose. Backwash interval was 7 hours. Filtration rate was 1.7 m/day (70.8 L/m^{2}h). Raw water-2 was used in this experiment.

Fig. 9 shows comparative plots of TMP versus the filtration time for direct and indirect pulse dose methods (Fig. 7S, SI) combined with a coagulation treatment (Methods B and C described in Figs. 3S and 4S, respectively). Analogous comparisons between SPAC and SSPAC are shown in Fig. 18S (SI). The indirect pulse dose method resulted in a more stable and lower TMP than the direct pulse dose method for both SPAC and SSPAC. With the indirect pulse dose method, water was manually shaken vigorously after the injection of the AC. With the direct pulse dose method, the AC was injected into the tank and mixed with raw water by bubbling for 3 min. The TMP was therefore lower with indirect dosing than with direct dosing because indirect pulse dosing produced a well-mixed AC suspension. The implication here is that complete dispersion of the AC before being deposited on the membrane is a key for a better precoating.

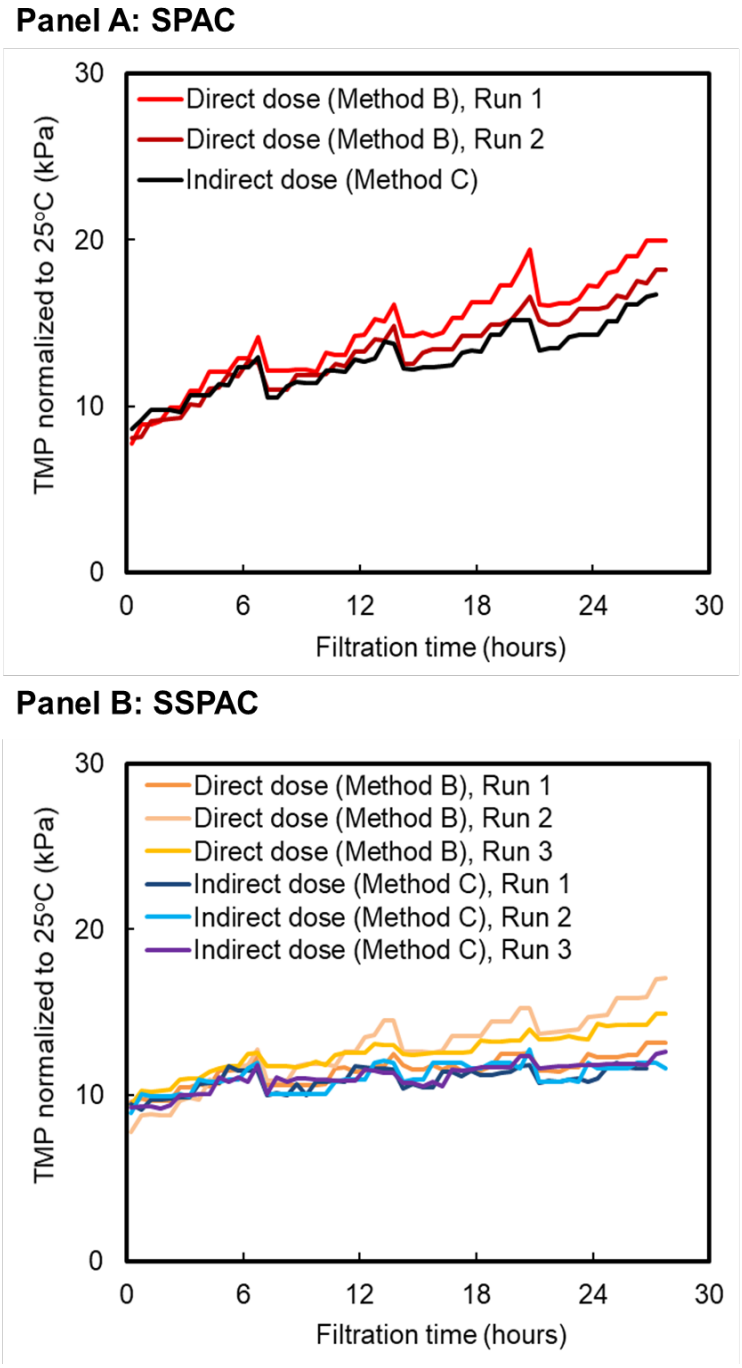

Fig. 9 —TMP as a function of filtration time when membrane filtration was conducted after SPAC/SSPAC adsorption and coagulation pretreatment. SPAC (Panel A) and SSPAC (Panel B) with direct pulse dose and indirect pulse dose (Method B and C, respectively, as explained in Figures 3S, 4S and 7S, SI) were used in this experiment. Backwash interval was 7 hours. Filtration rate was 1.7 m/day (70.8 L/m^2 h). Raw water-2 was used in this experiment.

3.5. Biopolymer and HS removal during AC addition and membrane filtration with backwash

During the filtration process, filtrate samples were taken and analyzed regarding the biopolymer and HS concentrations (Fig. 10). During experiments with a direct pulse dose but without coagulation, the removal was mostly higher for biopolymers than for HS. Biopolymer removal was improved by reducing the AC particle size and through coagulation pretreatment. The improvement of the removal was more apparent for biopolymers than for HS. The biopolymer concentrations in the filtrate were reduced by precoating with SSPAC, followed by SPAC and PAC. This order was the same as that of the TMP reduction (Fig. 5). During experiments with direct pulse SSPAC dosing without coagulation, the high percentage of biopolymer removal (75%) indicated that the biopolymers were removed primarily by the thin cake layer formed with SSPAC on top of the membrane before the biopolymers could reach and foul the membrane. However, the quantitative contributions of the coagulation, adsorption, and straining effects on the biopolymer removal, as well as the mitigation of the increase TMP, have yet to be investigated.

The fact that biopolymer removal was also higher with pulse SSPAC dosing than with continuous SSPAC dosing supports the merit of using a precoating to prevent membrane fouling. In the direct SSPAC pulse dosing experiments, biopolymer removal was higher without coagulation than with coagulation. This result was unexpected but can be explained if a denser deposition of SSPAC on the membrane without coagulation than with coagulation leads to a higher biopolymer removal. It should be noted, however, that without coagulation, the membrane was severely fouled by the AC itself (section 3.4).

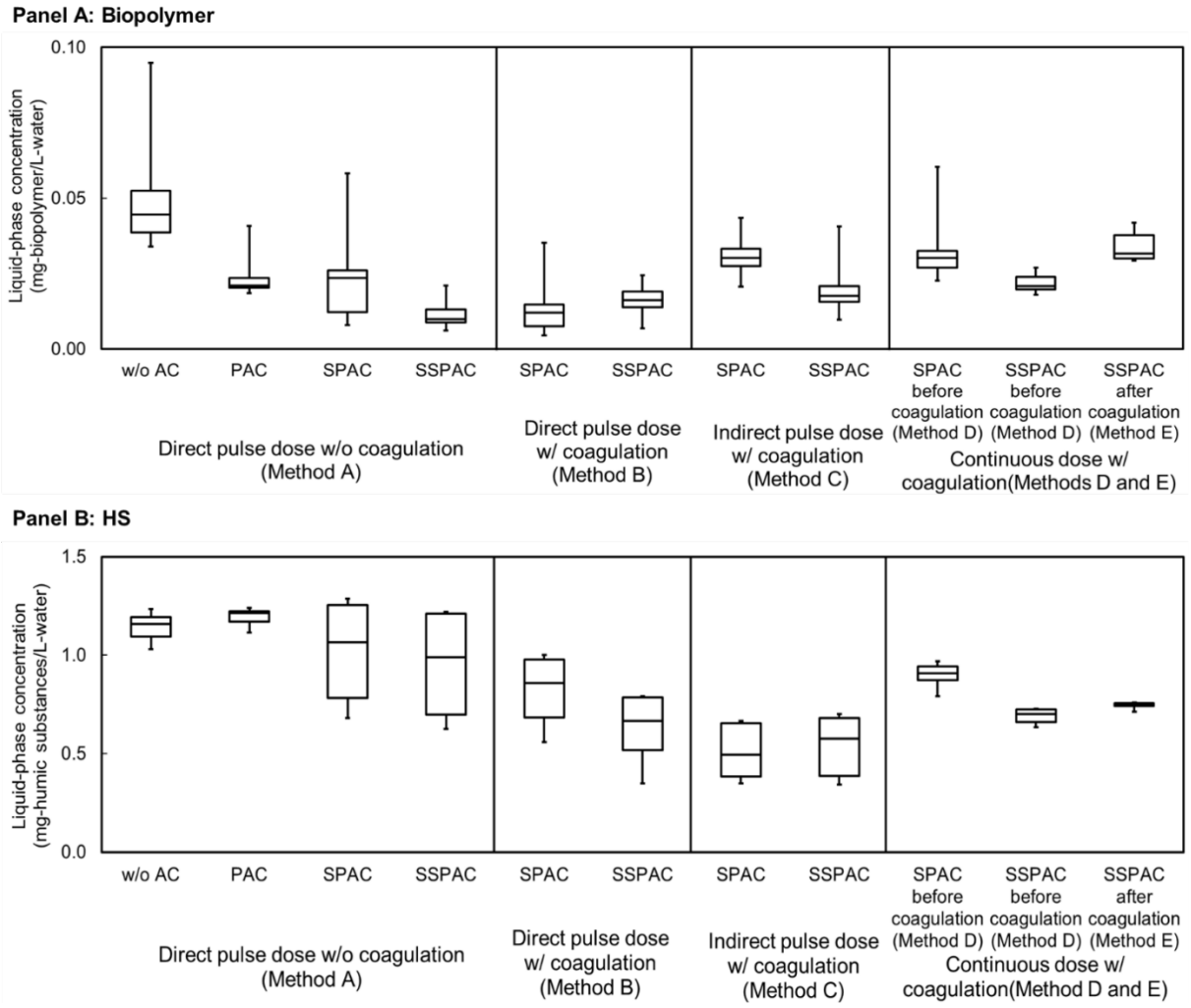

Fig. 10 — Box and whisker plots of biopolymers and humic substances (HS) concentrations in filtrates for different combinations of coagulation and powdered activated carbon (PAC) treatment. Horizontal lines within boxes represent median values, the upper and lower lines of the boxes represent the 75th and 25th percentiles, respectively, and the upper and lower bars outside the boxes indicate the maximum and minimum values, respectively.

4. Conclusions

(1) The capacity of AC to adsorb a biopolymer increases with a decrease in the AC particle size and hence follows the order PAC < SPAC < SSPAC. SSPAC selectively adsorbs a biopolymer from NOM compared with SPAC and PAC. The superiority of SSPAC for

biopolymer adsorption suggests that it has potential application in the control of membrane fouling.

(2) Biopolymers are also physically removed by a SPAC/SSPAC layer which precoats the membrane. The SSPAC precoating removes biopolymers through a better straining than SPAC; sonication can disperse agglomerated SPAC/SSPAC to produce a denser precoat and thereby enhance the straining effect.

(3) Coagulation is indispensable in the AC precoat filtration. Coagulation not only removes biopolymers it also facilitates the detachment of AC particles from the membrane during hydraulic backwashing, and in this way prevents hydraulically irreversible membrane fouling by AC.

(4) The pulse dosing of SSPAC (for precoating a submerged membrane) shows superiority in alleviating the buildup of TMP owing to hydraulically irreversible membrane fouling versus continuous dosing. The fact that an indirect pulse dosing of SSPAC preceded by coagulation pretreatment achieves the best prevention of an overall increase in the TMP indicates that AC dispersion is important for a precoating.

Acknowledgments

This work was supported by JSPS (Japan Society for the Promotion of Science) KAKENHI Grant Number JP16H06362. The authors gratefully acknowledge Futamura Chemical for providing PAC samples.

References

Adusei-Gyamfi, J., Ouddane, B., Rietveld, L., Cornard, J.P., Criquet, J., 2019. Natural organic matter-cations complexation and its impact on water treatment: A critical review. Water Res. 160, 130–147.

Amaral, P., Partlan, E., Li, M., Lapolli, F., Mefford, O.T., Karanfil, T., Ladner, D.A., 2016. Superfine powdered activated carbon (S-PAC) coatings on microfiltration membranes: Effects of milling time on contaminant removal and flux. Water Res. 100, 429–438.

Amy, G., 2008. Fundamental understanding of organic matter fouling of membranes. Desalination 231, 44–51.

Ando, N., Matsui, Y., Kurotobi, R., Nakano, Y., Matsushita, T., Ohno, K., 2010. Comparison of natural organic matter adsorption capacities of super-powdered activated carbon and powdered activated Carbon. Water Res. 44, 4127–4136.

Ando, N., Matsui, Y., Matsushita, T., Ohno, K., 2011. Direct observation of solid-phase adsorbate concentration profile in powdered activated carbon particle to elucidate mechanism of high adsorption capacity on super-powdered activated carbon. Water Res. 45, 761–767.

Ayache, C., Pidou, M., Croué, J.P., Labanowski, J., Poussade, Y., Tazi-Pain, A., Keller, J., Gernjak, W., 2013. Impact of effluent organic matter on low-pressure membrane fouling in tertiary treatment. Water Res. 47, 2633–2642.

Bonvin, F., Jost, L., Randin, L., Bonvin, E., Kohn, T., 2016. Super-fine powdered activated carbon (SPAC) for efficient removal of micropollutants from wastewater treatment plant effluent. Water Res. 90, 90–99.

Campinas, M., 2010. Assessing PAC contribution to the NOM fouling control in PAC/UF systems. Water Res. 44, 1636–1644.

Chen, F., Peldszus, S., Elhadidy, A.M., Legge, R.L., Van Dyke, M.I., Huck, P.M., 2016. Kinetics of natural organic matter (NOM) removal during drinking water biofiltration using different NOM characterization approaches. Water Res. 104, 361–370.

Cheng, X., Liang, H., Ding, A., Zhu, X., Tang, X., Gan, Z., Xing, J., Wu, D., Li, G., 2017. Application

585 of Fe(II)/peroxymonosulfate for improving ultrafiltration membrane performance in surface
586 water treatment: Comparison with coagulation and ozonation. Water Res. 124, 298–307.
587 Crittenden, J.C., Trussell, R.R., Hand, D.W., Howe, K.J., Tchobanoglous, G., 2012. MWH's water
588 treatment: principles and design. John Wiley & Sons.
589 Crozes, G., Anselme, C., Mallevialle, J., 1993. Effect of adsorption of organic matter on fouling of
590 ultrafiltration membranes. J. Memb. Sci. 84, 61–77.
591 Ding, Q., Yamamura, H., Yonekawa, H., Aoki, N., Murata, N., Hafuka, A., Watanabe, Y., 2018.
592 Differences in behaviour of three biopolymer constituents in coagulation with polyaluminium
593 chloride: Implications for the optimisation of a coagulation–membrane filtration process. Water
594 Res. 133, 255–263.
595 Fabris, R., Lee, E.K., Chow, C.W.K., Chen, V., Drikas, M., 2007. Pre-treatments to reduce fouling of
596 low pressure micro-filtration (MF) membranes. J. Memb. Sci. 289, 231–240.
597 Filloux, E., Gallard, H., Croue, J.P., 2012. Identification of effluent organic matter fractions
598 responsible for low-pressure membrane fouling. Water Res. 46, 5531–5540.
599 Filloux, E., Gernjak, W., Gallard, H., Croue, J.P., 2016. Investigating the relative contribution of
600 colloidal and soluble fractions of secondary effluent organic matter to the irreversible fouling of
601 MF and UF hollow fibre membranes. Sep. Purif. Technol. 170, 109–115.
602 Heijman, S.G.J., Hamad, J.Z., Kennedy, M.D., Schippers, J., Amy, G., 2009. Submicron powdered
603 activated carbon used as a pre-coat in ceramic micro-filtration. Desalin. Water Treat. 9, 86–91.
604 Huang, B.C., Guan, Y.F., Chen, W., Yu, H.Q., 2017. Membrane fouling characteristics and mitigation
605 in a coagulation-assisted microfiltration process for municipal wastewater pretreatment. Water
606 Res. 123, 216–223.
607 Huber, S.A., Balz, A., Abert, M., Pronk, W., 2011. Characterisation of aquatic humic and non-humic
608 matter with size-exclusion chromatography - organic carbon detection - organic nitrogen
609 detection (LC-OCD-OND). Water Res. 45, 879–885.
610 Jarvis, P., Sharp, E., Pidou, M., Molinder, R., Parsons, S.A., Jefferson, B., 2012. Comparison of
611 coagulation performance and floc properties using a novel zirconium coagulant against
612 traditional ferric and alum coagulants. Water Res. 46, 4179–4187.

613 Jung, C.W., Son, H.J., Kang, L.S., 2006. Effects of membrane material and pretreatment coagulation
614 on membrane fouling: fouling mechanism and NOM removal. Desalination 197, 154–164.
615 Kanaya, S., Kawase, Y., Mima, S., Sugiura, K., Murase, K., Yonekawa, H., 2015. Drinking water
616 treatment using superfine PAC (SPAC): Design and successful operation history in full-scale
617 plant. Am. Water Work. Assoc. Salt Lake City, Utah, USA, pp. 624–631.
618 Keeley, J., Jarvis, P., Smith, A.D., Judd, S.J., 2016. Coagulant recovery and reuse for drinking water
619 treatment. Water Res. 88, 502–509.
620 Kim, J., Cai, Z., Benjamin, M.M., 2008. Effects of adsorbents on membrane fouling by natural organic
621 matter. J. Memb. Sci. 310, 356–364.
622 Kimura, K., Maeda, T., Yamamura, H., Watanabe, Y., 2008. Irreversible membrane fouling in
623 microfiltration membranes filtering coagulated surface water. J. Memb. Sci. 320, 356–362.
624 Kimura, K., Oki, Y., 2017. Efficient control of membrane fouling in MF by removal of biopolymers:
625 Comparison of various pretreatments. Water Res. 115, 172–179.
626 Kimura, K., Shikato, K., Oki, Y., Kume, K., Huber, S.A., 2018. Surface water biopolymer
627 fractionation for fouling mitigation in low-pressure membranes. J. Memb. Sci. 554, 83–89.
628 Kimura, K., Tanaka, K., Watanabe, Y., 2014. Microfiltration of different surface waters with/without
629 coagulation: Clear correlations between membrane fouling and hydrophilic biopolymers. Water
630 Res. 49, 434–443.
631 Kweon, J.H., Hur, H.W., Seo, G.T., Jang, T.R., Park, J.H., Choi, K.Y., Kim, H.S., 2009. Evaluation of
632 coagulation and PAC adsorption pretreatments on membrane filtration for a surface water in
633 Korea: A pilot study. Desalination 249, 212–216.
634 Lee, J.-W., Choi, S.-P., Moon, H., Shim, W.-G., Thiruvenkatachari, R., 2006. Submerged
635 microfiltration membrane coupled with alum coagulation/powdered activated carbon adsorption
636 for complete decolorization of reactive dyes. Water Res. 40, 435–444.
637 Lee, N., Amy, G., Croué, J.P., Buisson, H., 2004. Identification and understanding of fouling in low-
638 pressure membrane (MF/UF) filtration by natural organic matter (NOM). Water Res. 38, 4511–
639 4523.
640 Lin, C.F., Huang, Y.J., Hao, O.J., 1999. Ultrafiltration processes for removing humic substances:

641 Effect of molecular weight fractions and PAC treatment. Water Res. 33, 1252–1264.
642 Lin, C.F., Liu, S.H., Hao, O.J., 2001. Effect of functional groups of humic substances on UF
643 performance. Water Res. 35, 2395–2402.
644 Luo, W., Arhatari, B., Gray, S.R., Xie, M., 2018. Seeing is believing: Insights from synchrotron
645 infrared mapping for membrane fouling in osmotic membrane bioreactors. Water Res. 137, 355–
646 361.
647 Ma, M., Liu, R., Liu, H., Qu, J., 2014. Mn(VII)-Fe(II) pre-treatment for Microcystis aeruginosa
648 removal by Al coagulation: Simultaneous enhanced cyanobacterium removal and residual
649 coagulant control. Water Res. 65, 73–84.
650 Matsui, Y., Aizawa, T., Kanda, F., Nigorikawa, N., Mima, S., Kawase, Y., 2007. Adsorptive removal
651 of geosmin by ceramic membrane filtration with super-powdered activated carbon. J. Water
652 Supply Res. Technol. - AQUA 56, 411–418.
653 Matsui, Y., Ando, N., Yoshida, T., Kurotobi, R., Matsushita, T., Ohno, K., 2011. Modeling high
654 adsorption capacity and kinetics of organic macromolecules on super-powdered activated carbon.
655 Water Res. 45, 1720–1728.
656 Matsui, Y., Fukuda, Y., Inoue, T., Matsushita, T., Aoki, N., Mima, S., 2004. Enhancing an adsorption-
657 membrane hybrid system with microground activated carbon. Water Sci. Technol. Water Supply
658 4, 189–197.
659 Matsui, Y., Hasegawa, H., Ohno, K., Matsushita, T., Mima, S., Kawase, Y., Aizawa, T., 2009. Effects
660 of super-powdered activated carbon pretreatment on coagulation and trans-membrane pressure
661 buildup during microfiltration. Water Res. 43, 5160–5170.
662 Matsui, Y., Murase, R., Sanogawa, T., Aoki, N., Mima, S., Inoue, T., Matsushita, T., 2005. Rapid
663 adsorption pretreatment with submicrometre powdered activated carbon particles before
664 microfiltration. Water Sci. Technol. 51, 249–256.
665 Matsui, Y., Nakao, S., Taniguchi, T., Matsushita, T., 2013. Geosmin and 2-methylisoborneol removal
666 using superfine powdered activated carbon: Shell adsorption and branched-pore kinetic model
667 analysis and optimal particle size. Water Res. 47, 2873–2880.
668 Matsui, Y., Sakamoto, A., Nakao, S., Taniguchi, T., Matsushita, T., Shirasaki, N., Sakamoto, N.,

669 Yurimoto, H., 2014. Isotope microscopy visualization of the adsorption profile of 2-
670 methylisoborneol and geosmin in powdered activated carbon. Environ. Sci. Technol. 48, 10897–
671 10903.
672 Matsui, Y., Sanogawa, T., Aoki, N., Mima, S., Matsushita, T., 2006. Evaluating submicron-sized
673 activated carbon adsorption for microfiltration pretreatment. Water Sci. Technol. Water Supply
674 6, 149–155.
675 Myat, D.T., Stewart, M.B., Mergen, M., Zhao, O., Orbell, J.D., Gray, S., 2014. Experimental and
676 computational investigations of the interactions between model organic compounds and
677 subsequent membrane fouling. Water Res. 48, 108–118.
678 Pan, L., Matsui, Y., Matsushita, T., Shirasaki, N., 2016. Superiority of wet-milled over dry-milled
679 superfine powdered activated carbon for adsorptive 2-methylisoborneol removal. Water Res.
680 102, 516–523.
681 Pan, L., Nishimura, Y., Takaesu, H., Matsui, Y., Matsushita, T., Shirasaki, N., 2017. Effects of
682 decreasing activated carbon particle diameter from 30 Mm to 140 nm on equilibrium adsorption
683 capacity. Water Res. 124, 425–434.
684 Peiris, R.H., Jaklewicz, M., Budman, H., Legge, R.L., Moresoli, C., 2013. Assessing the role of feed
685 water constituents in irreversible membrane fouling of pilot-scale ultrafiltration drinking water
686 treatment systems. Water Res. 47, 3364–3374.
687 Su, Z., Liu, T., Yu, W., Li, X., Graham, N.J.D., 2017. Coagulation of surface water: Observations on
688 the significance of biopolymers. Water Res. 126, 144–152.
689 Tian, J., Ernst, M., Cui, F., Jekel, M., 2013. Correlations of relevant membrane foulants with UF
690 membrane fouling in different waters. Water Res. 47, 1218–28.
691 Umar, M., Roddick, F., Fan, L., 2016. Impact of coagulation as a pre-treatment for UVC/H2O2-
692 biological activated carbon treatment of a municipal wastewater reverse osmosis concentrate.
693 Water Res. 88, 12–19.
694 Wang, S., Liu, C., Li, Q., 2013. Impact of polymer flocculants on coagulation-microfiltration of
695 surface water. Water Res. 47, 4538–4546.
696 Wang, X.M., Li, X.Y., 2008. Accumulation of biopolymer clusters in a submerged membrane

bioreactor and its effect on membrane fouling. Water Res. 42, 855–862.

Wang, Y., Tng, K.H., Wu, H., Leslie, G., Waite, T.D., 2014. Removal of phosphorus from wastewaters using ferrous salts - A pilot scale membrane bioreactor study. Water Res. 57, 140–150.

Weiss, V.U., Golesne, M., Friedbacher, G., Alban, S., Szymanski, W.W., Marchetti-Deschmann, M., Allmaier, G., 2018. Size and molecular weight determination of polysaccharides by means of nano electrospray gas-phase electrophoretic mobility molecular analysis (nES GEMMA). Electrophoresis 39, 1142–1150.

Wray, H.E., Andrews, R.C., 2014. Optimization of coagulant dose for biopolymer removal: Impact on ultrafiltration fouling and retention of organic micropollutants. J. Water Process Eng. 1, 74–83.

Xing, J., Liang, H., Xu, S., Chuah, C.J., Luo, X., Wang, T., Wang, J., Li, G., Snyder, S.A., 2019. Organic matter removal and membrane fouling mitigation during algae-rich surface water treatment by powdered activated carbon adsorption pretreatment: Enhanced by UV and UV/chlorine oxidation. Water Res. 159, 283–293.

Ye, M., Zhang, H., Wei, Q., Lei, H., Yang, F., Zhang, X., 2006. Study on the suitable thickness of a PAC-precoated dynamic membrane coupled with a bioreactor for municipal wastewater treatment. Desalination 194, 108–120.

Yu, W., Liu, Teng, Crawshaw, J., Liu, Ting, Graham, N., 2018. Ultrafiltration and nanofiltration membrane fouling by natural organic matter: Mechanisms and mitigation by pre-ozonation and pH. Water Res. 139, 353–362.

Zheng, X., Ernst, M., Huck, P.M., Jekel, M., 2010. Biopolymer fouling in dead-end ultrafiltration of treated domestic wastewater. Water Res. 44, 5212–5221.

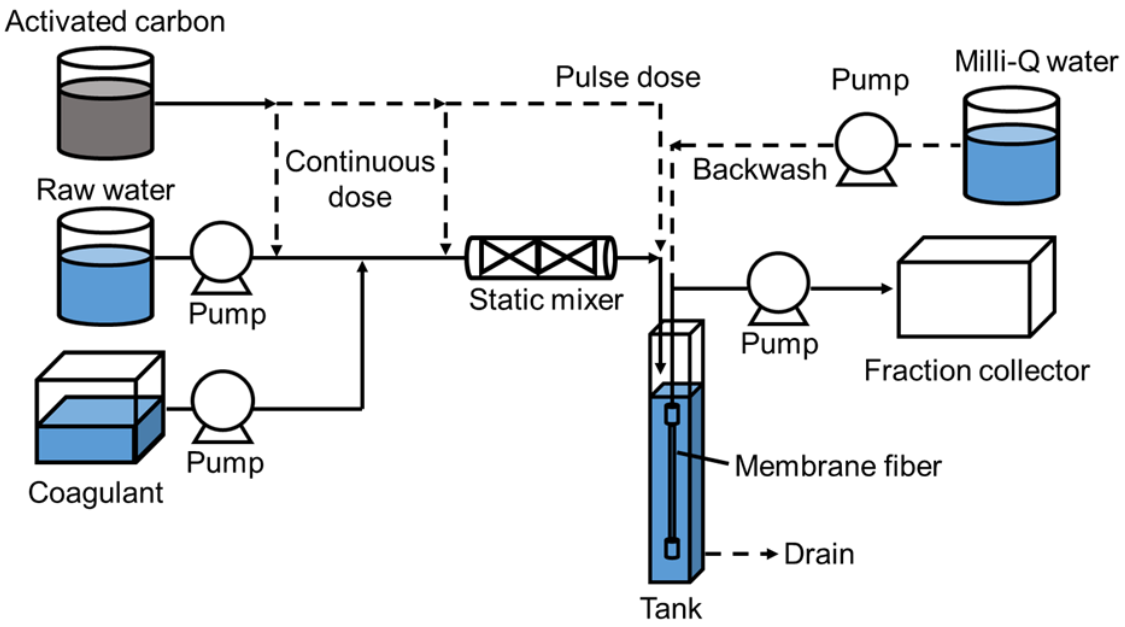

Fig. 1 — Laboratory setup for additions of activated carbon and coagulant and for submerged membrane filtration with backwash.

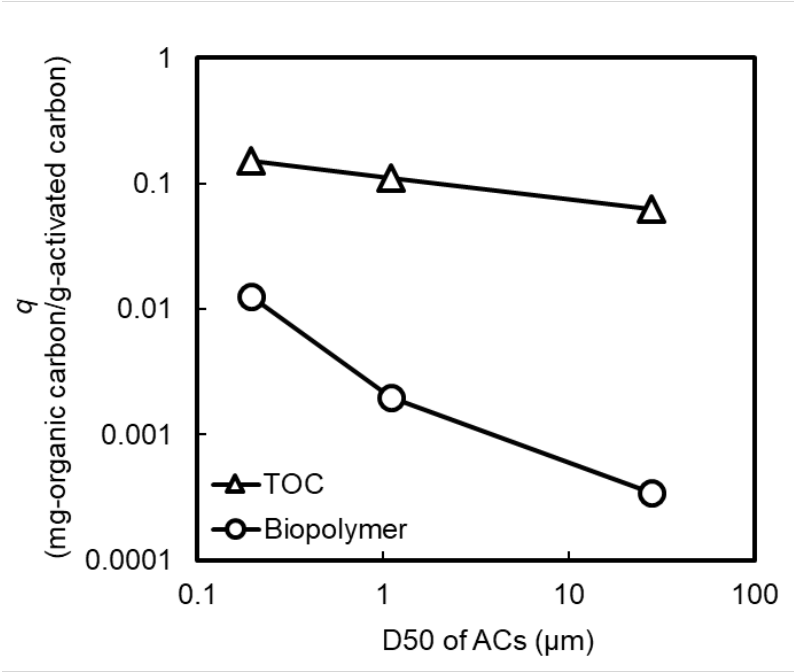

Fig. 2 — Plots of solid-phase concentration (*q*) at an equilibrium liquid-phase total organic carbon (TOC) concentration of 1.8 mg/L and a biopolymer concentration of 0.02 mg/L versus the median diameter (D50) of the activated carbons (ACs). The data are taken from Figs. 8S and 9S, SI. Raw water-2 was used in this experiment.

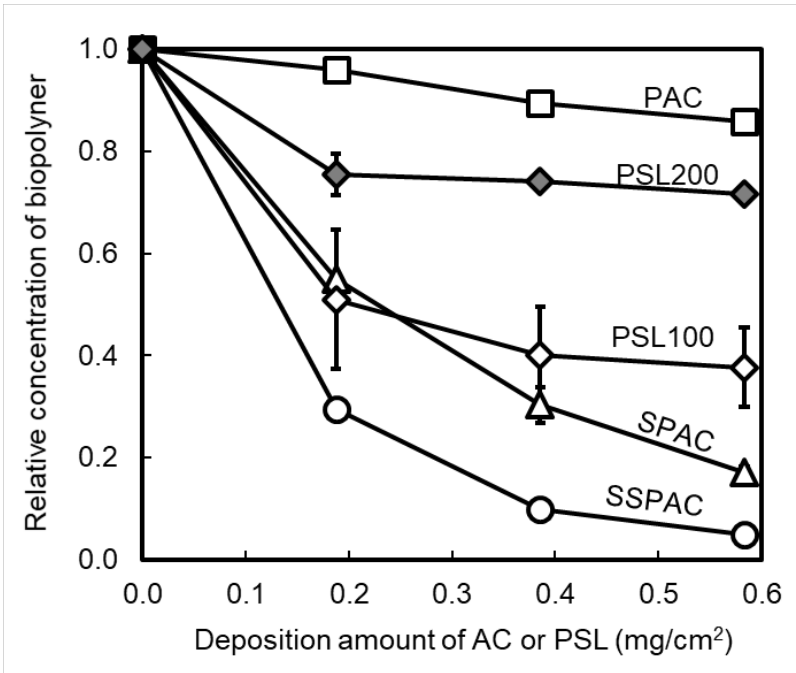

Fig. 3 — Fractions of biopolymers that remained after passing through a precoated membrane versus amounts of activated carbon (AC) or polystyrene latex spheres (PSLs) precoating the membrane. Biopolymer concentration was determined for 50-mL filtrate samples taken after precoating by filtering a 40-mL sample. Error bars indicate ranges of two measurements by liquid chromatography-organic carbon detection methodology. Raw water-1 was used in this experiment.

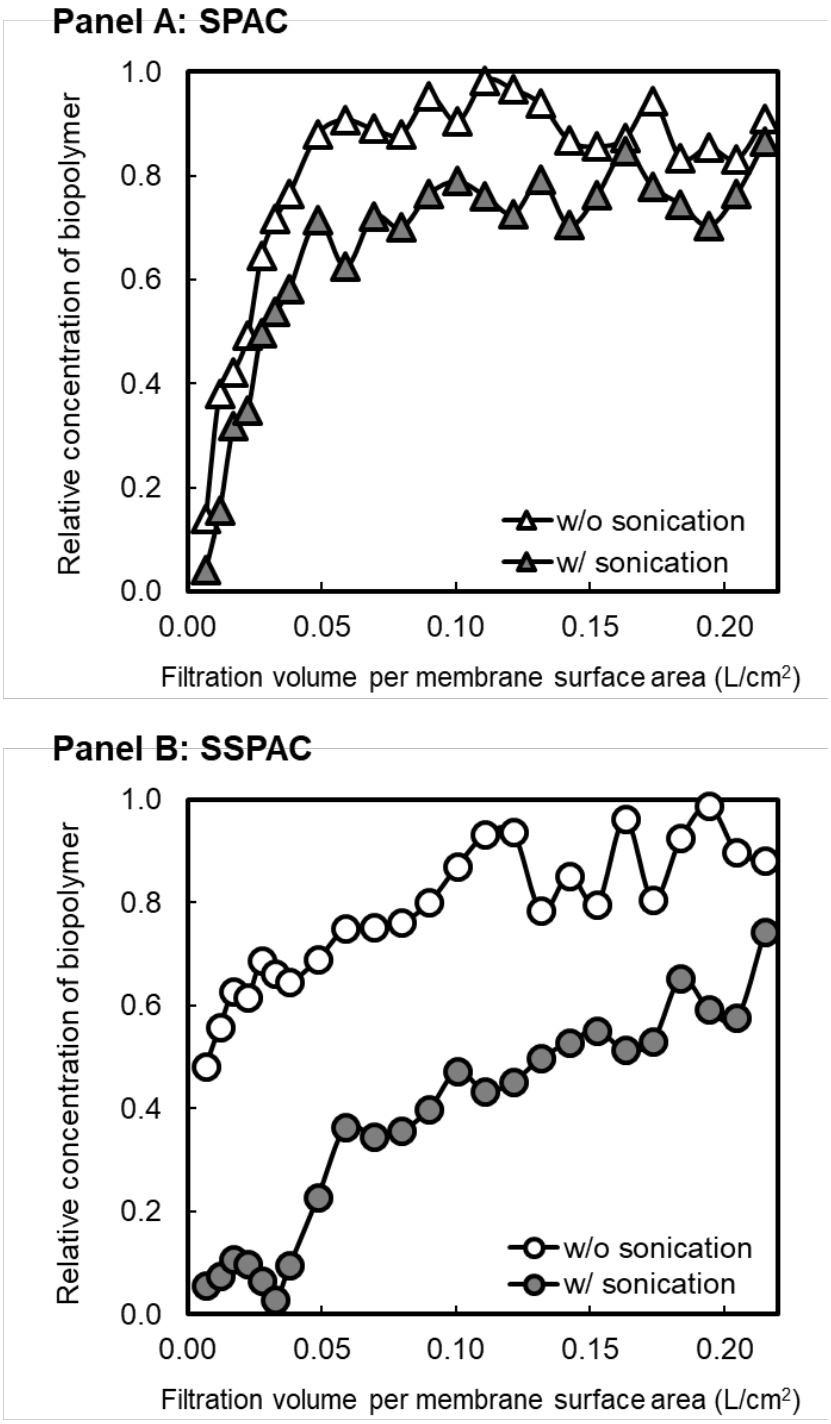

Fig. 4 — Relative concentration of biopolymer versus filtration volume per membrane surface area of water samples. The amount of powdered activated carbon (PAC) deposited on the membrane for precoating was 0.38 mg/cm^2. Panel A: SPAC. Panel B: SSPAC. Raw water-1 was used in this experiment.

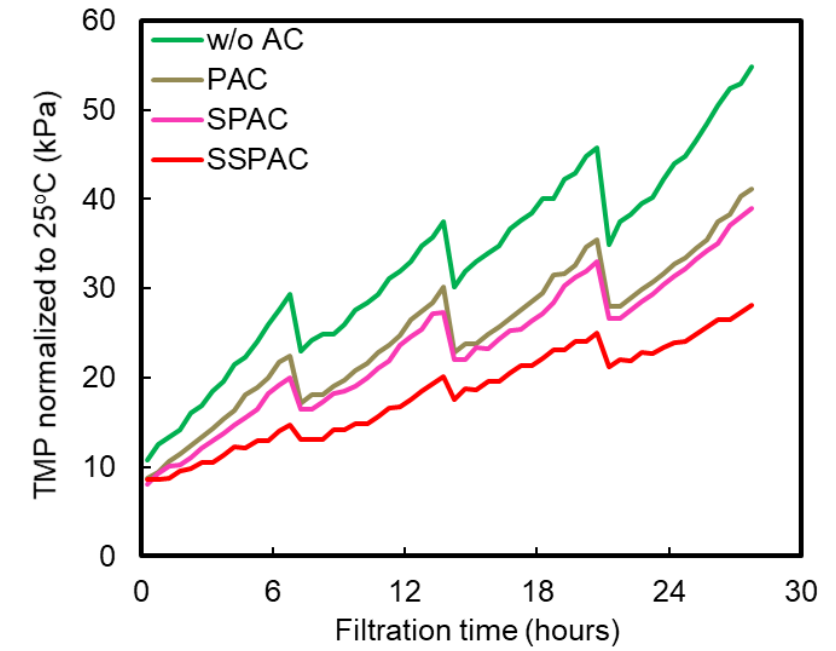

Fig. 5 — TMP versus filtration time for powdered activated carbon (PAC), superfine PAC (SPAC), and submicron SPAC (SSPAC). The experiments were conducted by Method A, where direct pulse dosing (explained in Figs. 2S and 7S, SI) was used. Backwash interval was 7 hours. Filtration rate was 1.7 m/day (70.8 L/m^{2}h). Raw water-2 was used in this experiment.

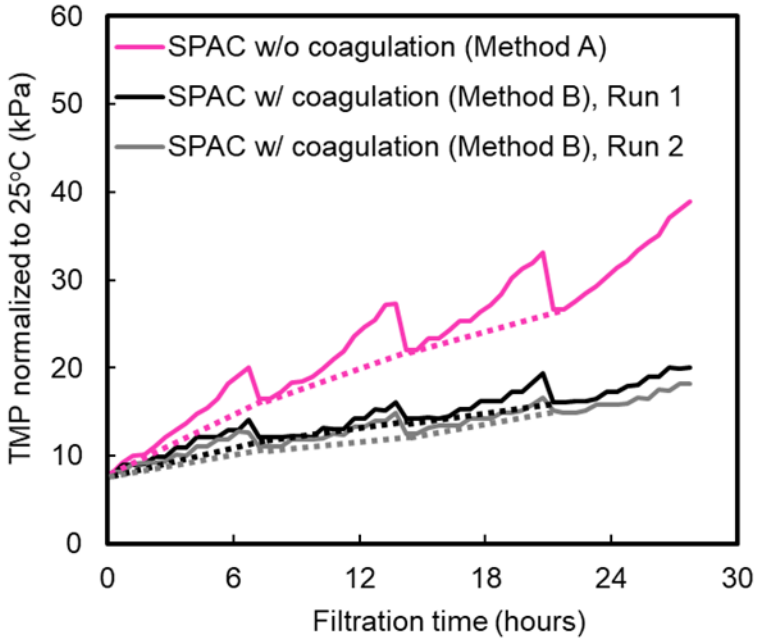

Fig. 6 — TMP versus filtration time with/without coagulation. The experiments were conducted by Methods A and B, where direct pulse dosing (explained in Figs. 2S, 3S and 7S, SI) of superfine powdered activated carbon (SPAC) was used. Dotted lines show TMP rise due to hydraulically irreversible fouling. Backwash interval was 7 hours. Filtration rate was 1.7 m/day (70.8 L/m^2 h). Raw water-2 was used in this experiment.

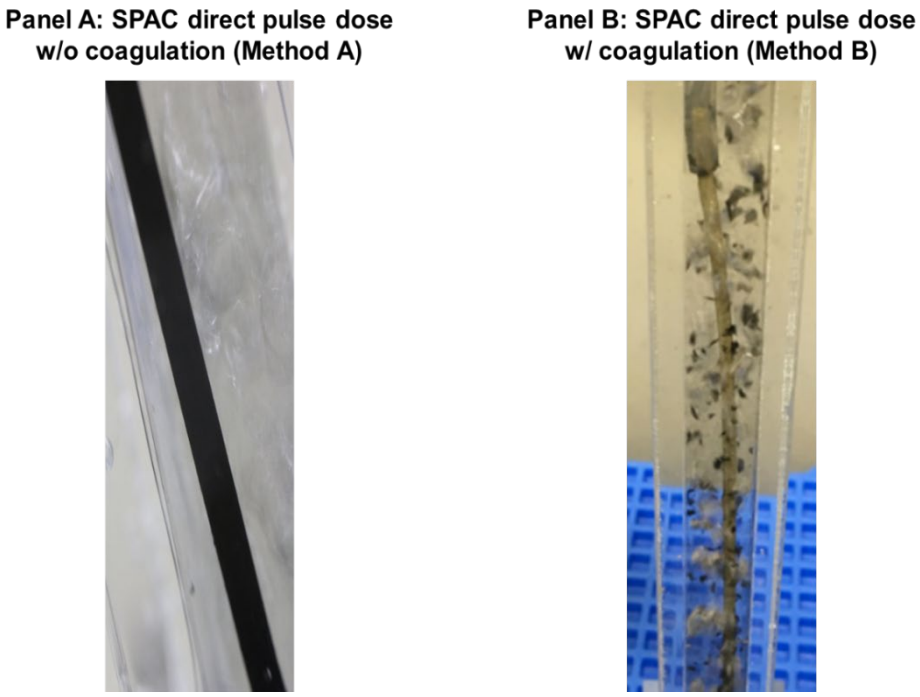

Fig. 7 — Photographs of a membrane tank during backwash. Panel A is a picture of the system without coagulation pretreatment (Method A). Panel B is a picture of the system with coagulation pretreatment (Method B). Direct pulse dosing (explained in Figs. 2S, 3S, and 7S, SI) was used in the experiments. Backwash pressure was 50 kPa. Filtration rate was 1.7 m/day (70.8 L/m^2 h). Raw water-2 was used in this experiment.

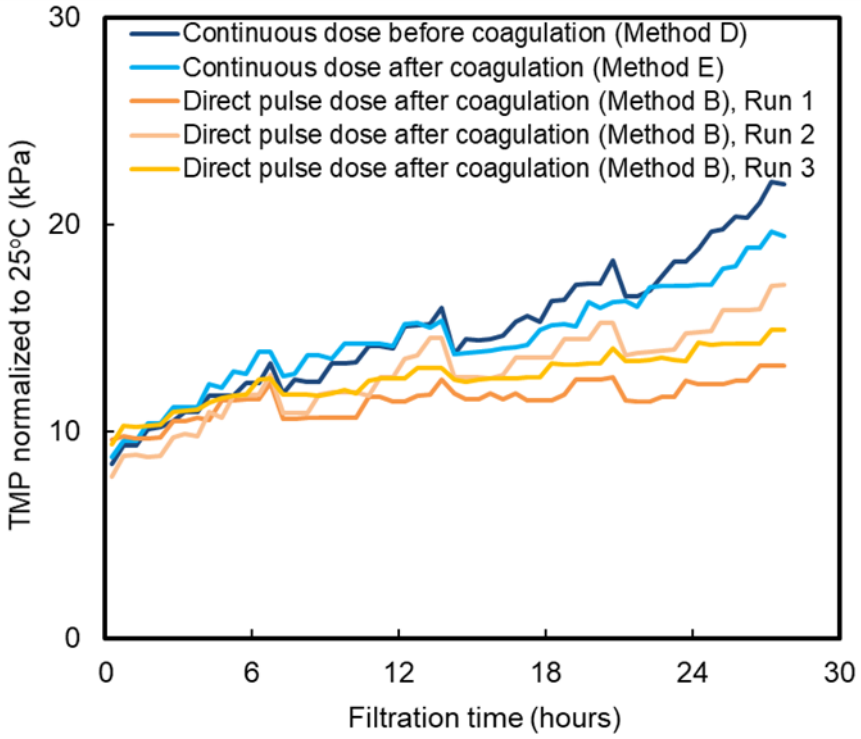

Fig. 8 —TMP as a function of filtration time when membrane filtration was conducted after SSPAC adsorption and coagulation pretreatment. The experiments were conducted by Methods B, D, and E (explained in Figs. 3S, 5S, and 6S, respectively, SI) to compare direct pulse dose and continues dose. Backwash interval was 7 hours. Filtration rate was 1.7 m/day (70.8 L/m^{2}h). Raw water-2 was used in this experiment.

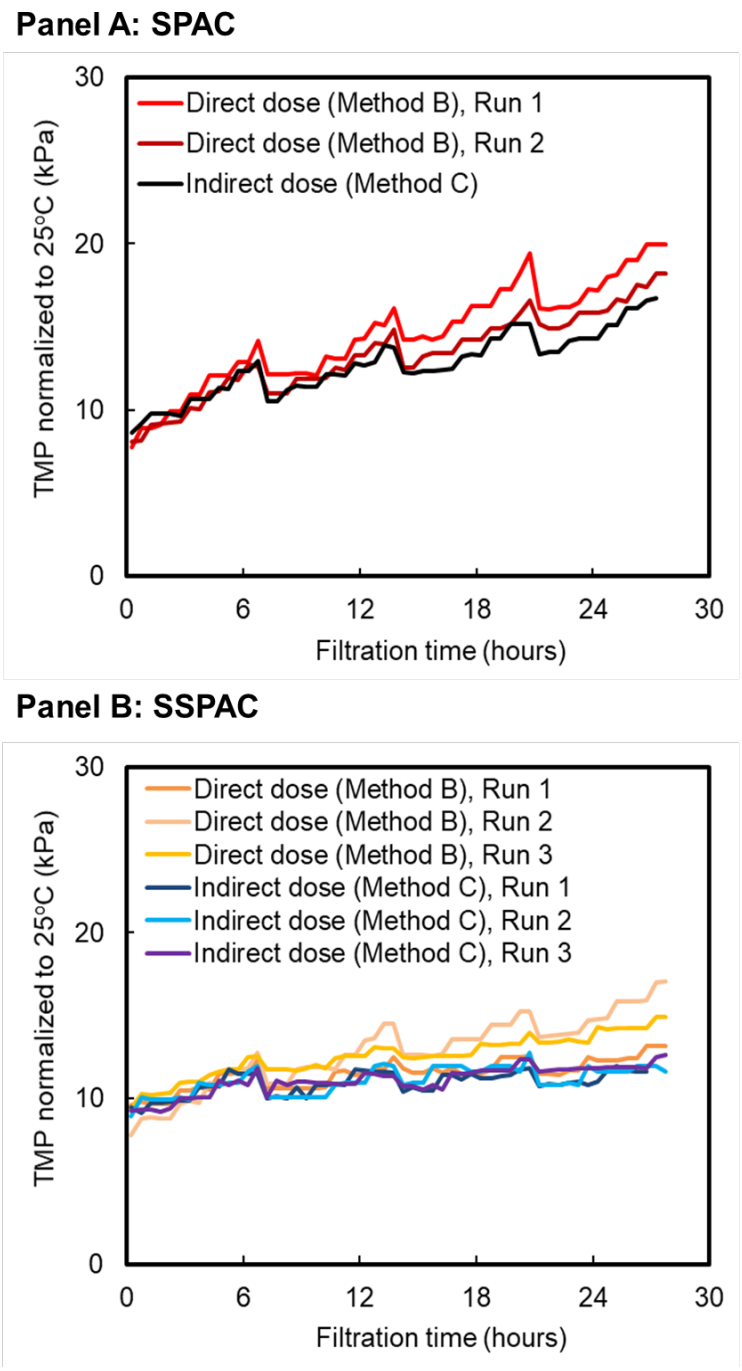

Fig. 9 —TMP as a function of filtration time when membrane filtration was conducted after SPAC/SSPAC adsorption and coagulation pretreatment. SPAC (Panel A) and SSPAC (Panel B) with direct pulse dose and indirect pulse dose (Method B and C, respectively, as explained in Figures 3S, 4S and 7S, SI) were used in this experiment. Backwash interval was 7 hours. Filtration rate was 1.7 m/day (70.8 L/m^2 h). Raw water-2 was used in this experiment.

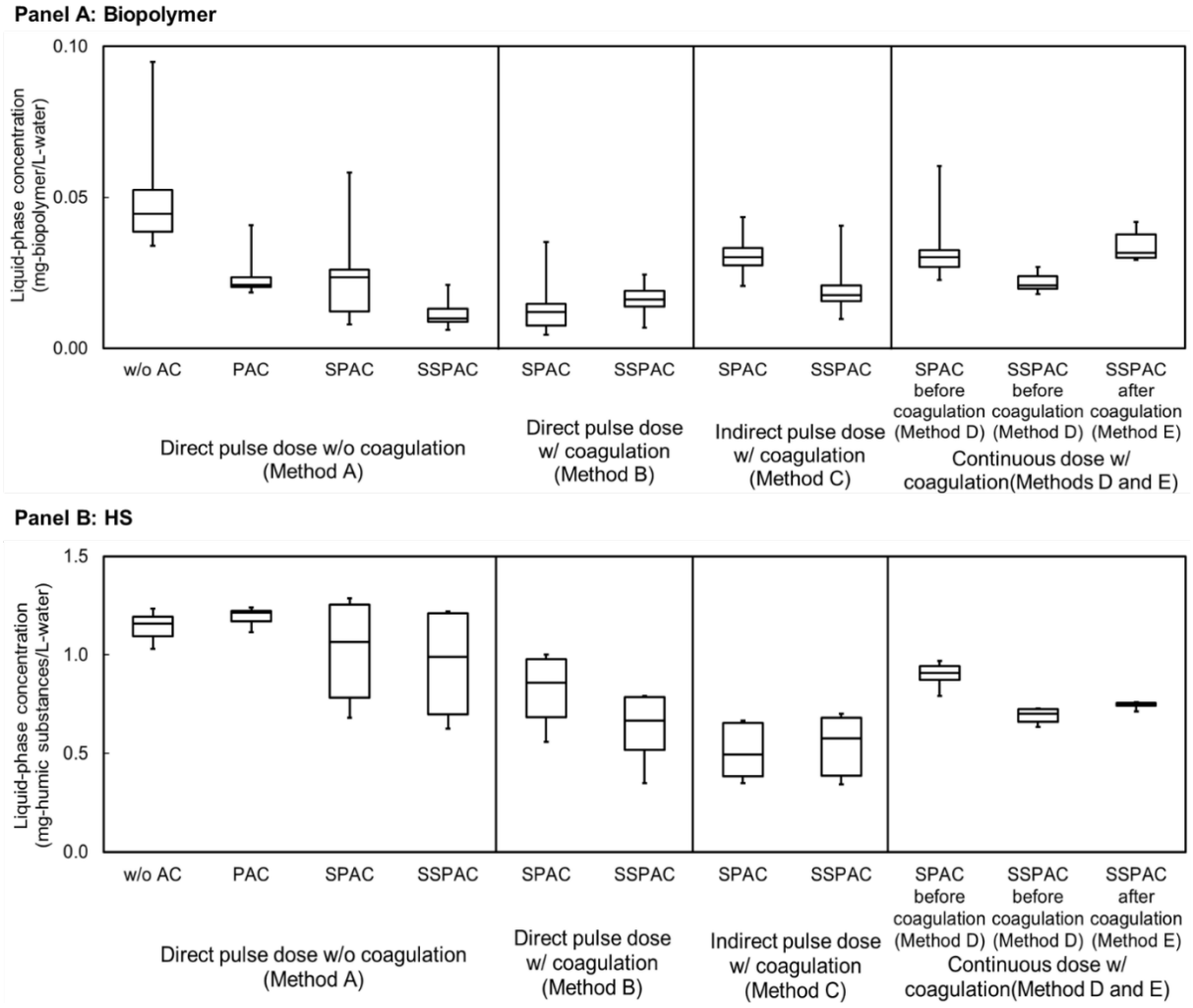

Fig. 10 — Box and whisker plots of biopolymers and humic substances (HS) concentrations in filtrates for different combinations of coagulation and powdered activated carbon (PAC) treatment. Horizontal lines within boxes represent median values, the upper and lower lines of the boxes represent the 75th and 25th percentiles, respectively, and the upper and lower bars outside the boxes indicate the maximum and minimum values, respectively.

Supplementary Information

Precoating membranes with submicron super-fine powdered activated carbon after coagulation prevents transmembrane pressure rise: Straining and high adsorption capacity effects

Yuanjun Zhao [a], Ryosuke Kitajima [a], Nobutaka Shirasaki [b], Yoshihiko Matsui [b], Taku Matsushita [b]*

[a] *Graduate School of Engineering, Hokkaido University.*
N13W8 Sapporo 060-8628 Japan
[b] *Faculty of Engineering, Hokkaido University*
N13W8 Sapporo 060-8628 Japan

* *Corresponding author*. Tel./fax: +81-11-706-7280
E-mail address: matsui@eng.hokudai.ac.jp (Y. Matsui)

Tab. 1S — Water quality of Raw water-1 and Raw water-2 (Raw water was pre-filtrated by 0.1-μm MCE membrane).

	pH	TOC (mg/L)	UV260 (cm^{-1})	Biopolymer (mg/L)	Alkalinity (mg/L as $CaCO_3$)	Na^+ (mg/L)	K^+ (mg/L)
Raw water-1	8.07	2.61	0.06	0.0725	71	52.7	6.03
Raw water-2	7.62	2.66	0.06	0.0770	72	43.7	5.84

	Mg^{2+} (mg/L)	Ca^{2+} (mg/L)	Cl^- (mg/L)	NO_3^- (mg/L)	SO_4^{2-} (mg/L)
Raw water-1	11.0	19.0	70.7	13.3	24.4
Raw water-2	9.18	18.0	54.0	13.8	22.3

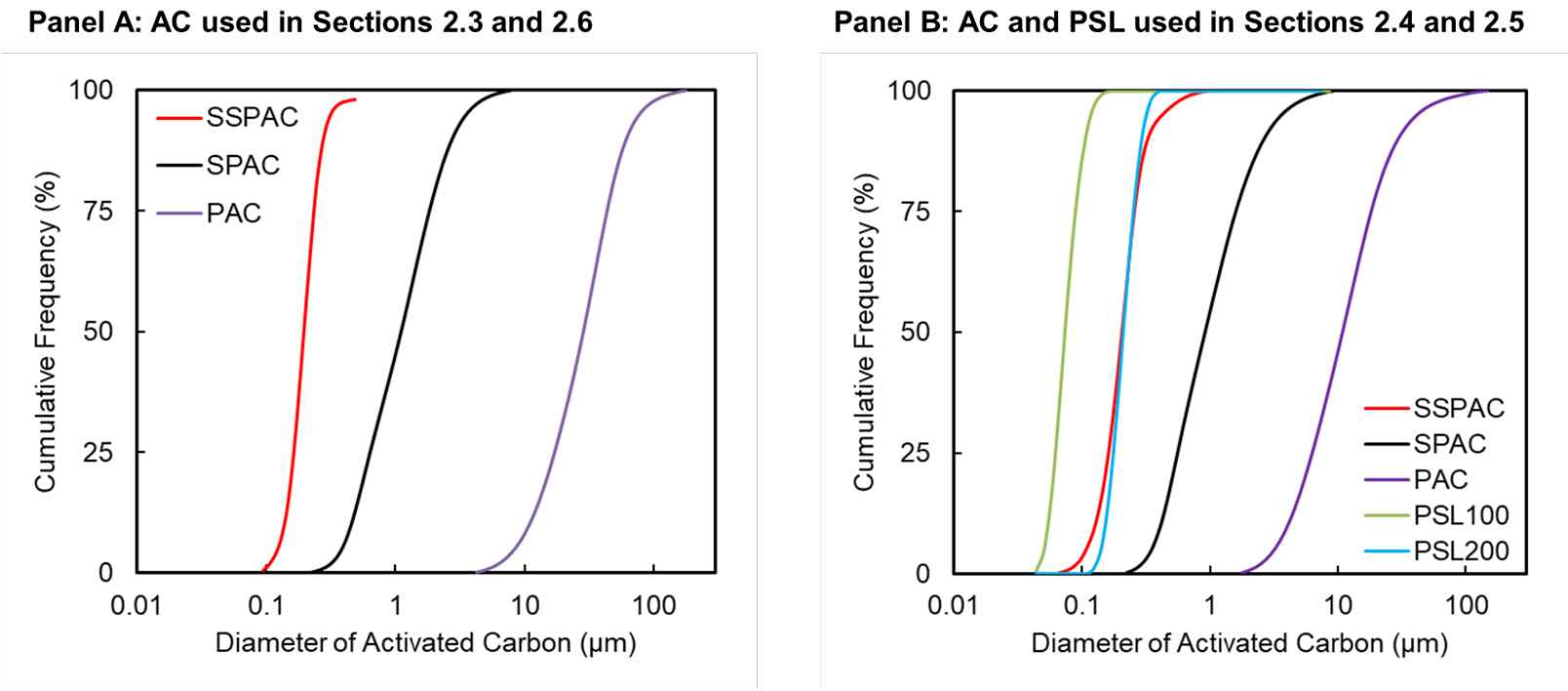

Fig. 1S — Size distributions of PAC (powdered activated carbon) and PSL (polystyrene latex) particles.

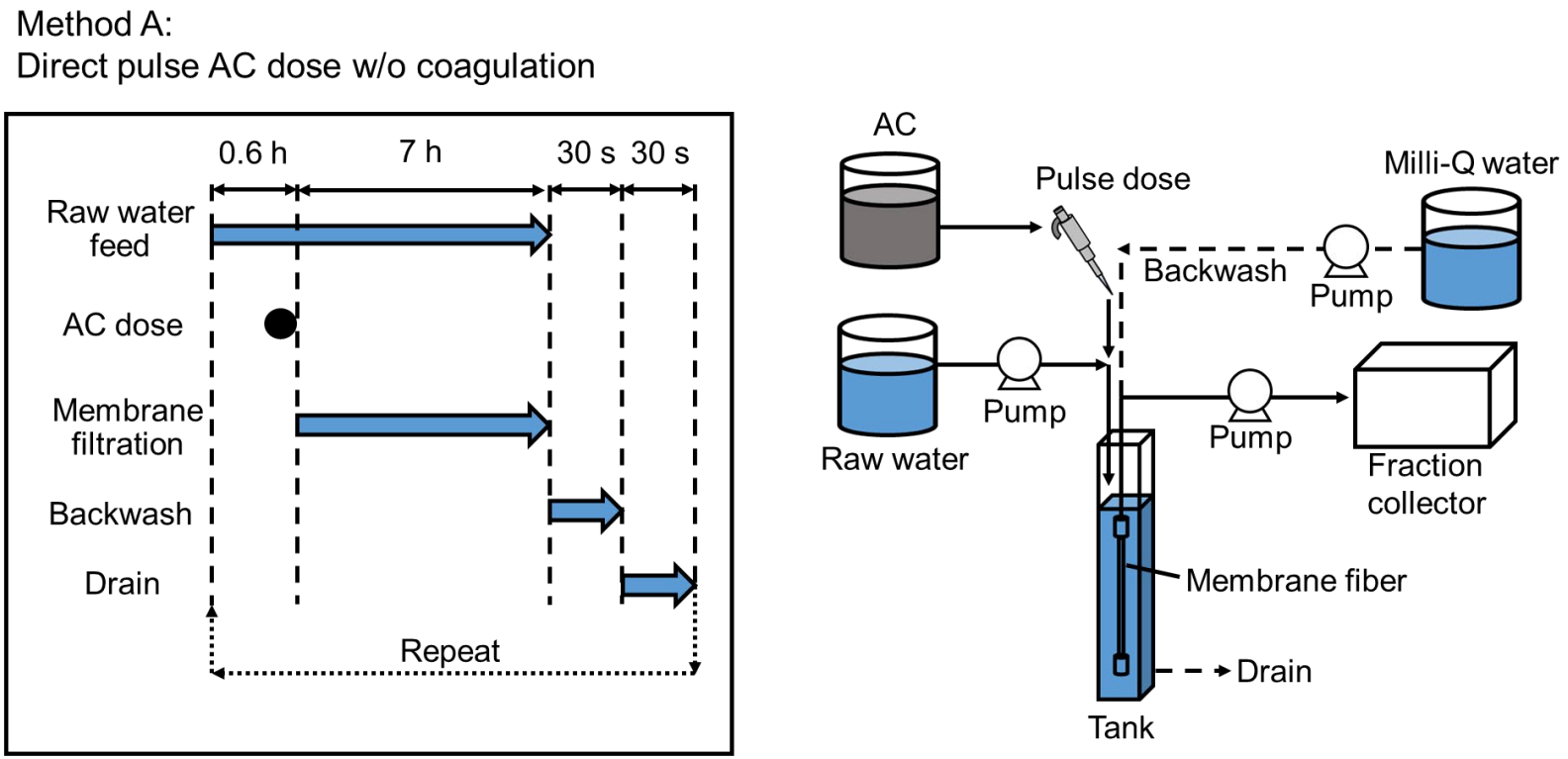

Fig. 2S —Method A: Process flow and time flow of the direct pulse AC dose without coagulation. (The process was repeated four rounds in every experiment)

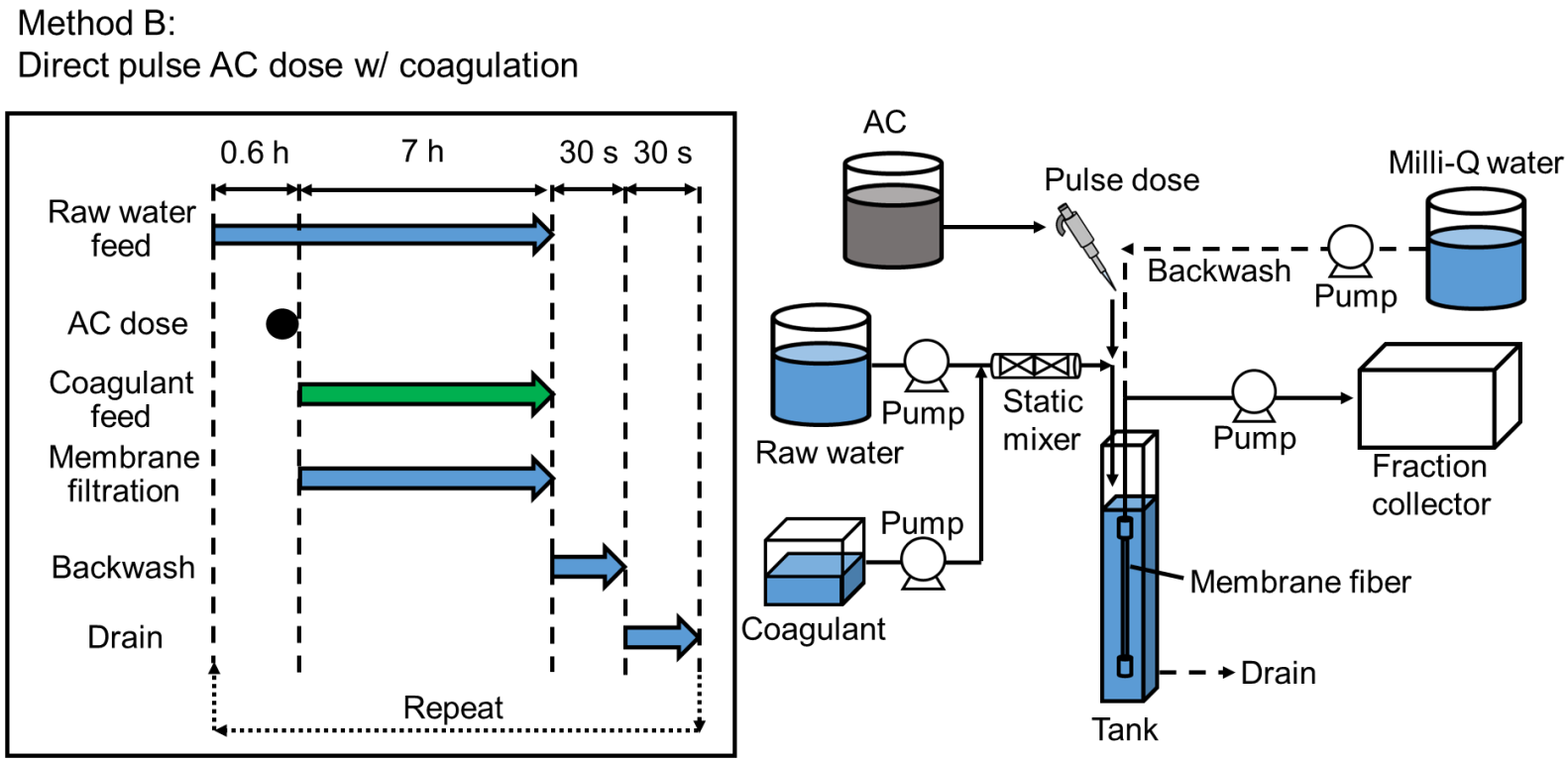

Fig. 3S —Method B: Process flow and time flow of the direct pulse AC dose with coagulation. (The process was repeated four rounds in every experiment)

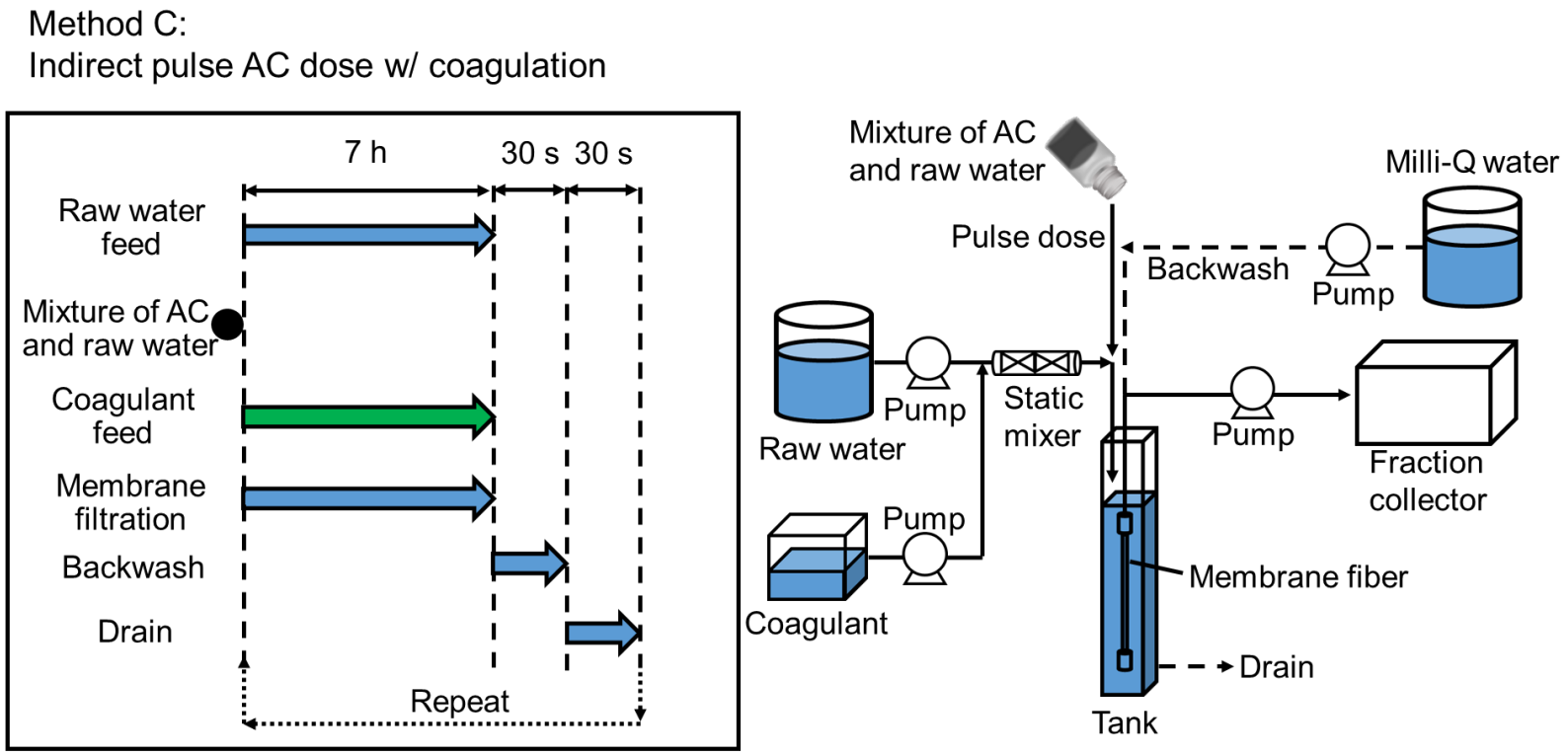

Fig. 4S —Method C: Process flow and time flow of the indirect pulse AC dose with coagulation. (The process was repeated four rounds in every experiment)

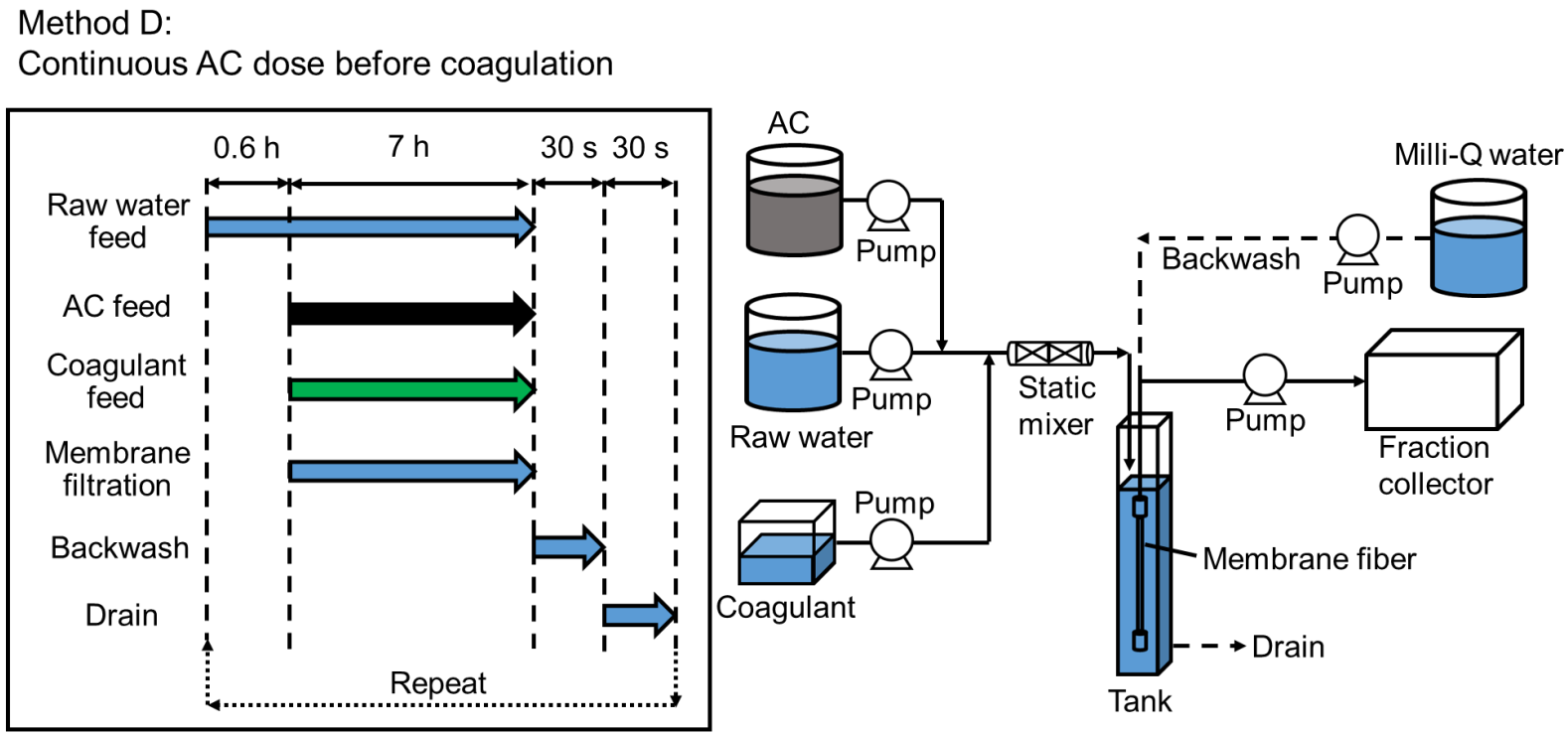

Fig. 5S —Method D: Process flow and time flow of continuous AC dose before coagulation. (The process was repeated four rounds in every experiment)

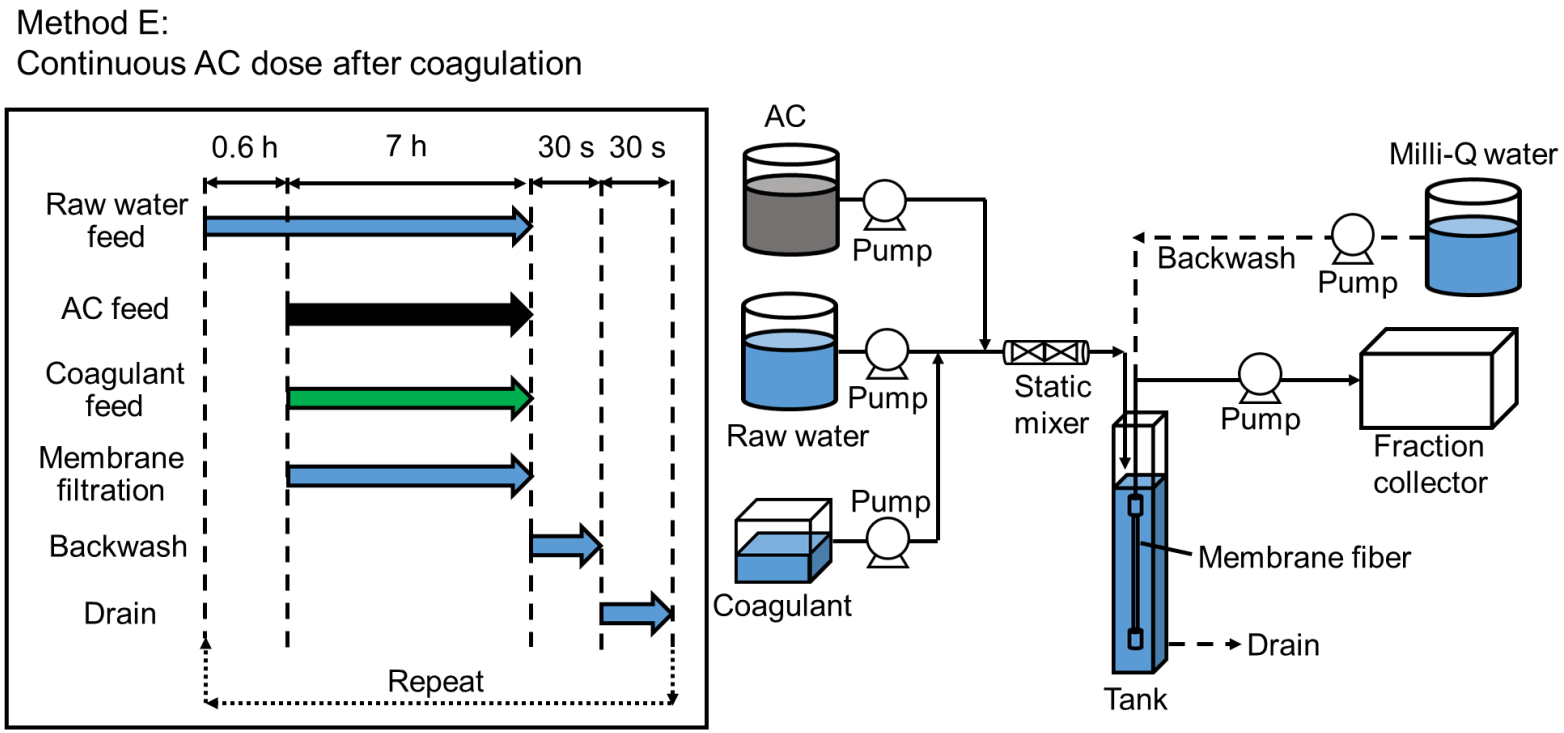

Fig. 6S —Method E: Process flow and time flow of continuous AC dose after coagulation. (The process was repeated four rounds in every experiment)

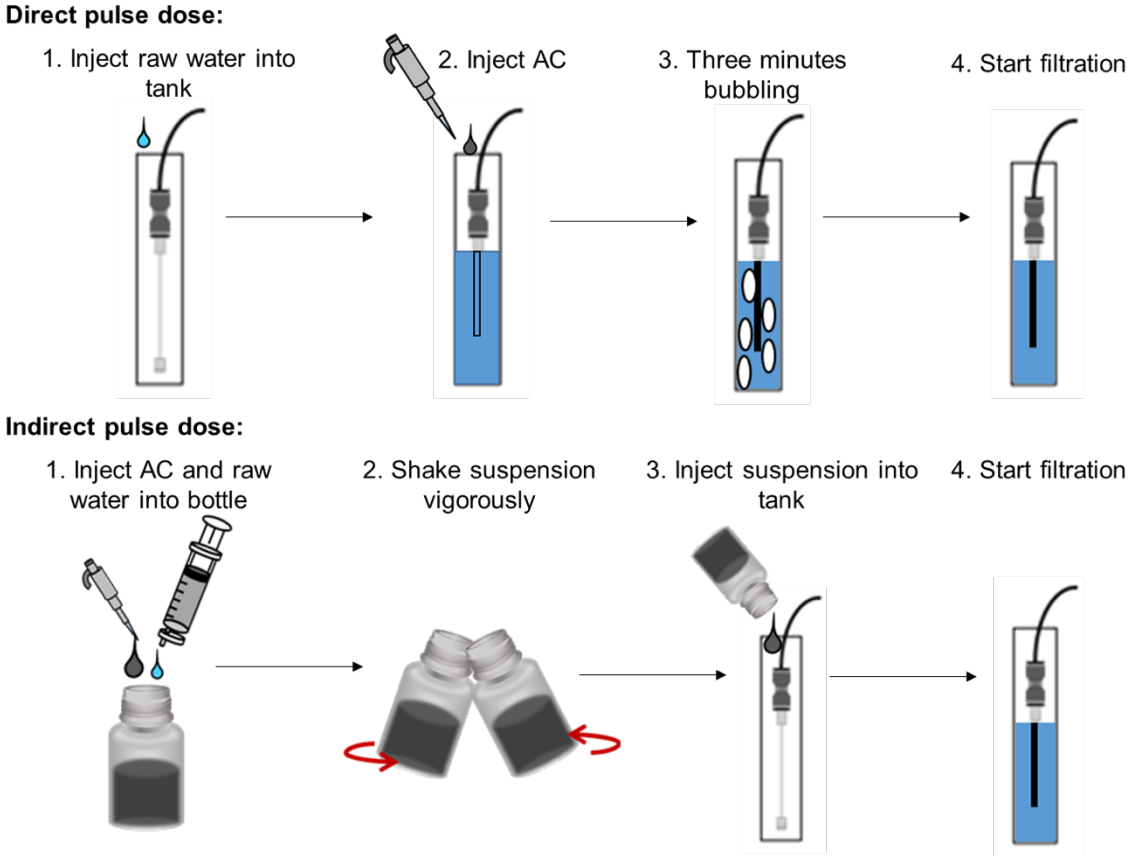

Fig. 7S — Direct and indirect pulse dose method explanation.

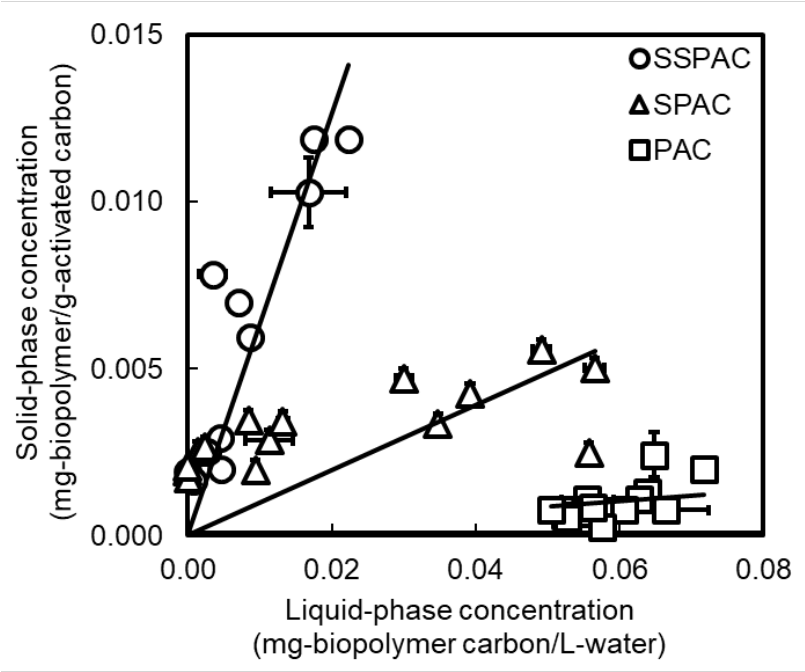

Fig. 8S — Solid-phase concentration versus liquid-phase concentration of biopolymer for different forms of powdered activated carbon (PAC). Raw water-2 was used in this experiment. The symbols indicate the data points. The lines are regression lines with an intercept of 0. The error bars indicate ranges of two measurements by liquid chromatography–organic carbon detection methodology (for the *x* axis) and consequent changes of calculated concentrations (for the *y* axis). Error bars indicate standard deviations of measurements. Some error bars are hidden behind the symbols.

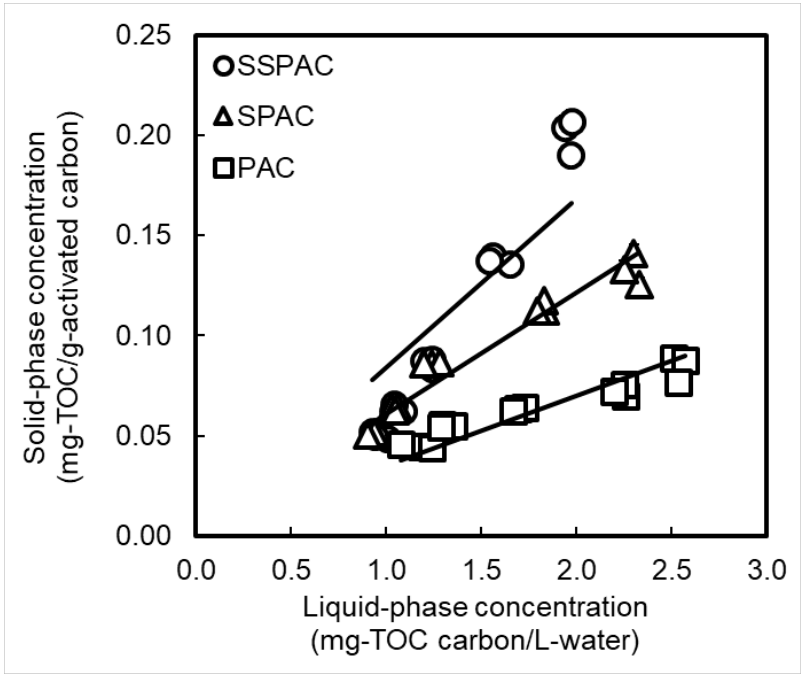

Fig. 9S — Solid-phase concentration versus liquid-phase concentration of total organic carbon (TOC) for different forms of powdered activated carbon (PAC). Raw water-2 was used in this experiment. The lines are regression lines with an intercept of 0. Error bars, which indicate standard deviations of measurements, are hidden by the plots.

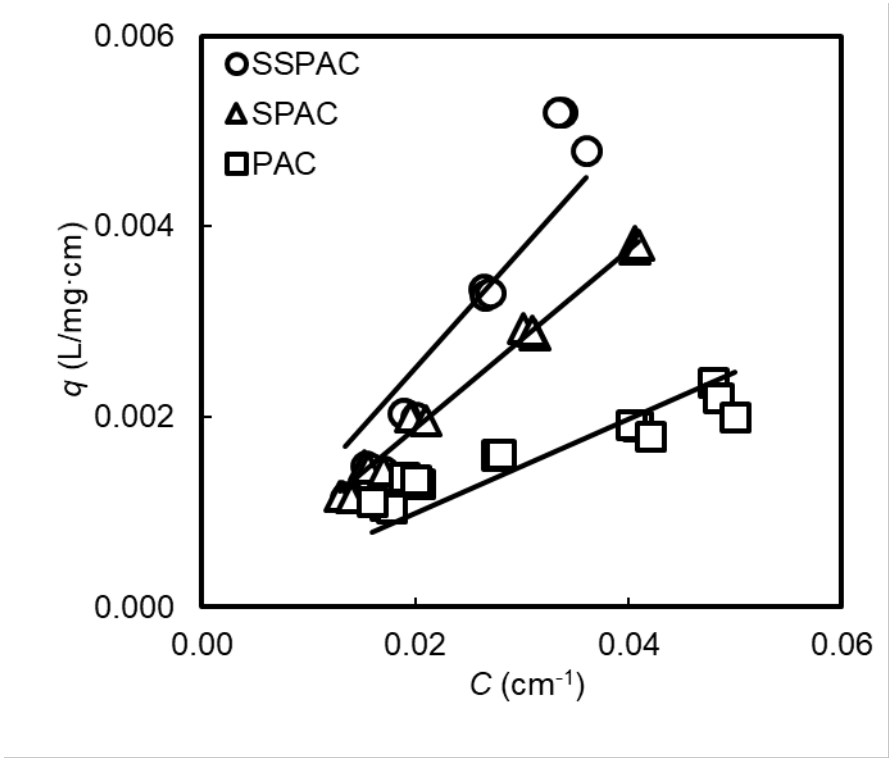

Fig. 10S — Solid-phase concentration (*q*) versus liquid-phase concentration (*C*) of UV260 for different forms of powdered activated carbon (PAC). Raw water-2 was used in this experiment. The lines are regression lines with an intercept of 0.

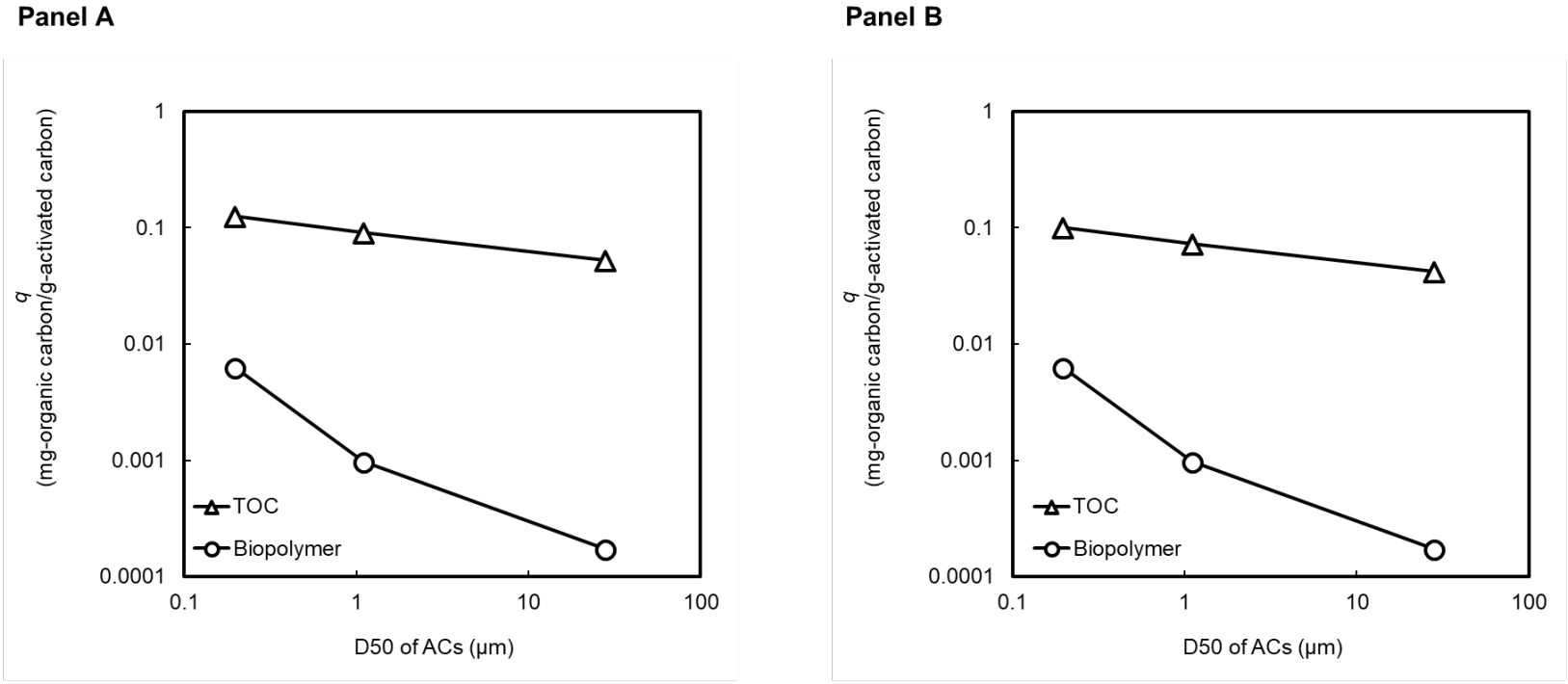

Fig. 11S — Plots of solid-phase concentration (*q*) at equilibrium with liquid-phase concentration of 1.5 mg/L of total organic carbon (TOC) and 0.01 mg/L of biopolymer (Panel A) and 1.2 mg/L TOC and 0.01 mg/L biopolymer (Panel B) versus median diameter (D50) of ACs (PAC, SPAC, and SSPAC). The data are taken from Figs. 8S and 9S. Raw water-2 was used in this experiment.

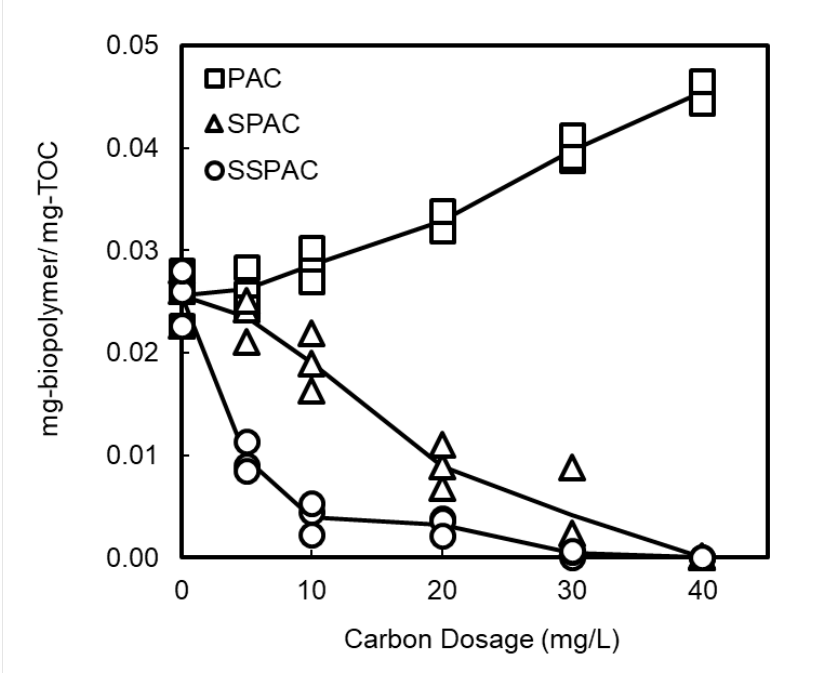

Fig. 12S — Biopolymer/total organic carbon (TOC) mass ratio versus carbon dosage for different kinds of powdered activated carbon (PAC). Raw water-2 was used in this experiment.

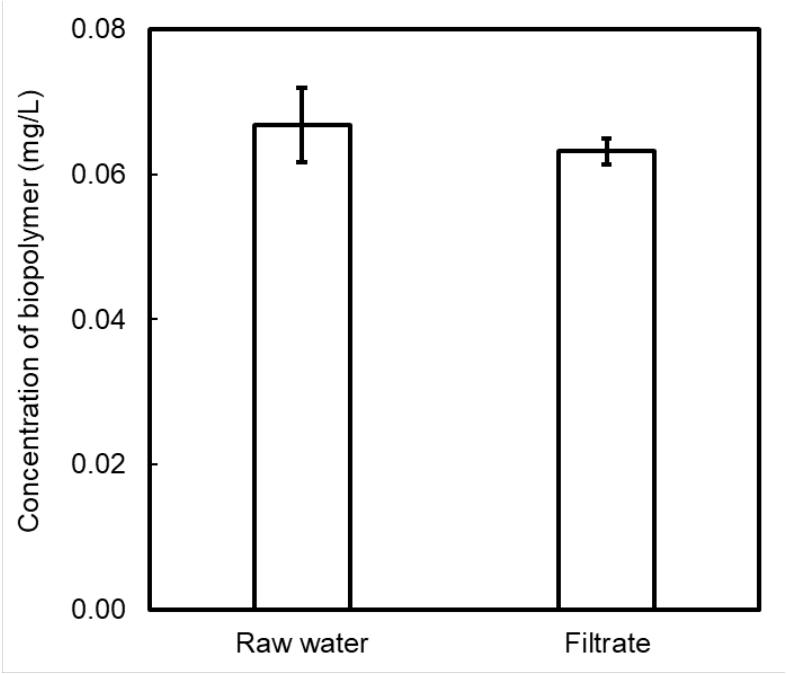

Fig. 13S — Biopolymer concentrations of water samples before and after passing through a membrane with a pore size of 0.1 µm. Raw water-2, which was prepared by filtration through a 0.1-µm pore-size membrane, was used in this filtration experiment. Error bars indicate standard deviations of measurements.

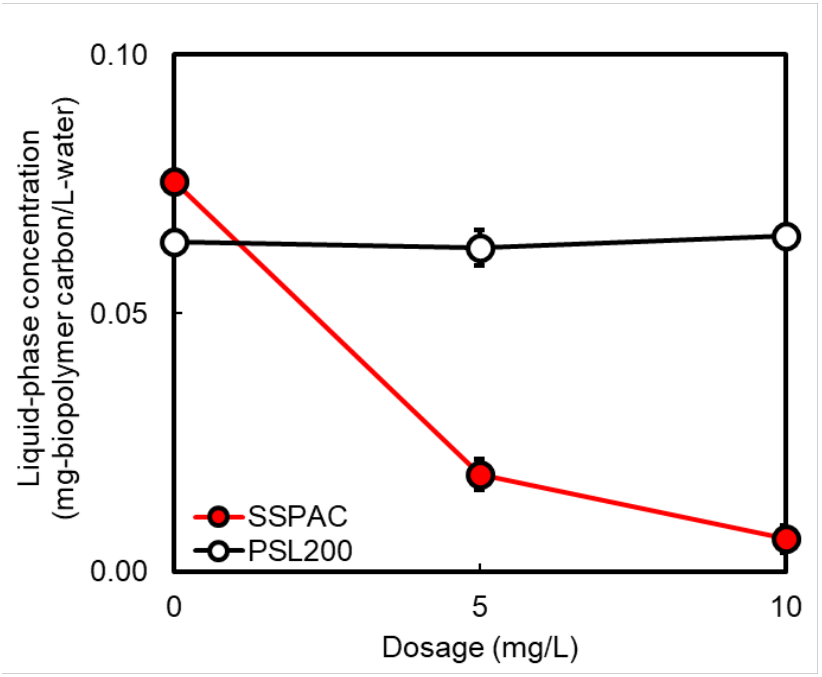

Fig. 14S — Liquid-phase concentration of biopolymer versus SSPAC (submicron superfine powdered activated carbon) and PSL200 (polystyrene latex of diameter 200 nm) dosages. Raw water-2 was used in this experiment. Error bars indicate standard deviations of measurements.

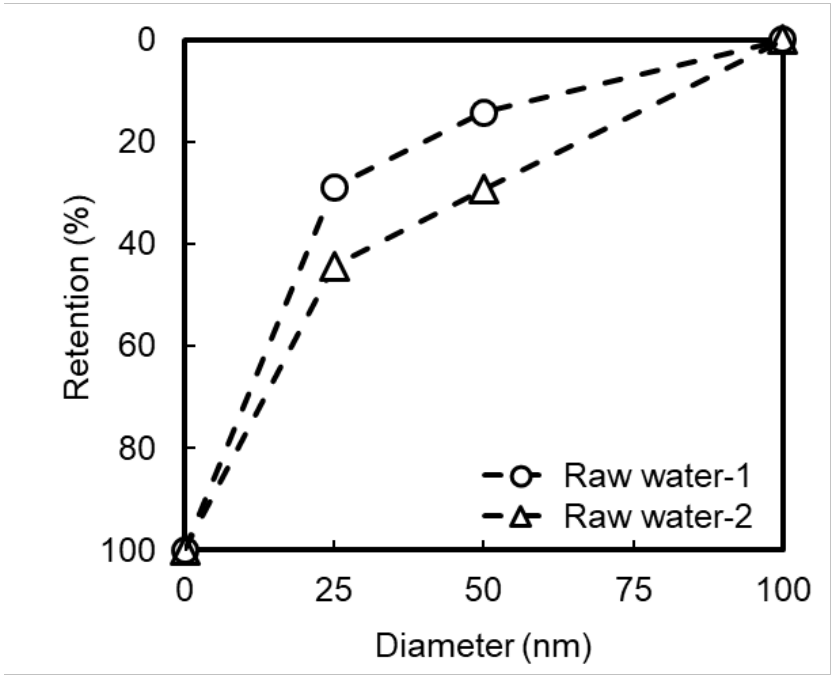

Fig. 15S — Retention of biopolymer vs. membrane pore diameter. MCE membrane filters (ϕ47 mm, Merck KGaA, Darmstadt, Germany) were used.

Panel A: SSPAC direct pulse dose w/o coagulation (Method A)

Panel B: SSPAC direct pulse dose w/ coagulation (Method B)

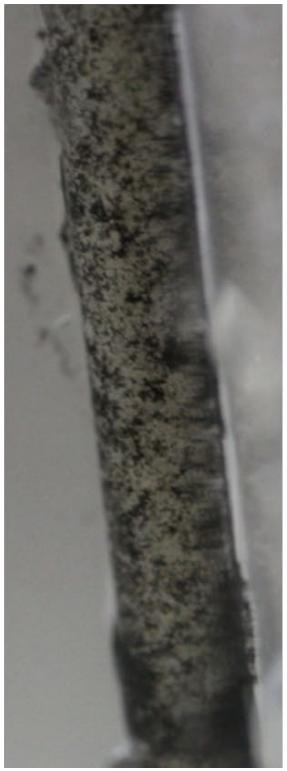

Fig. 16S — Photographs of a membrane tank during backwash. Panel A is a picture of the system without coagulation pretreatment (Method A). Panel B is a picture of the system with coagulation pretreatment (Method B). Direct pulse dosing (explained in Figs. 2S, 3S, and 7S, SI) was used in the experiments. Backwash pressure was 50 kPa. Filtration rate was 1.7 m/day (70.8 L/m^{2}h). Raw water-2 was used in this experiment.

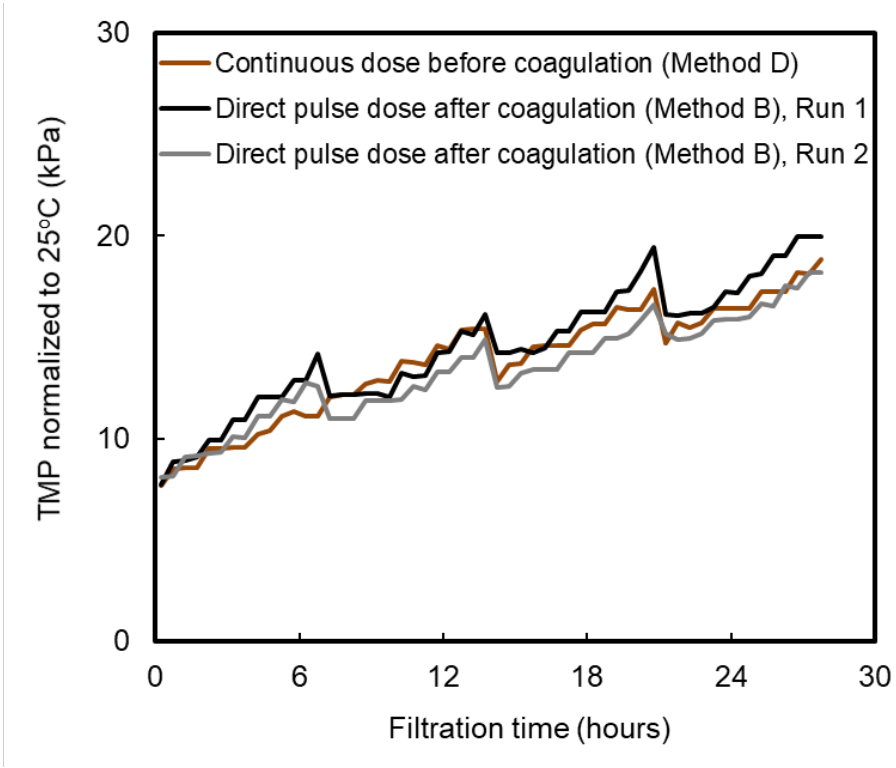

Fig. 17S —TMP as a function of filtration time when membrane filtration was conducted after SPAC (superfine powdered activated carbon) adsorption and coagulation pretreatment. The experiments were conducted by Methods B and D (explained in Figs. 3S and 5S, respectively, SI) to compare direct pulse dose and continues dose. Backwash interval was 7 hours. Filtration rate was 1.7 m/day (70.8 L/m^{2}h). Raw water-2 was used in this experiment.

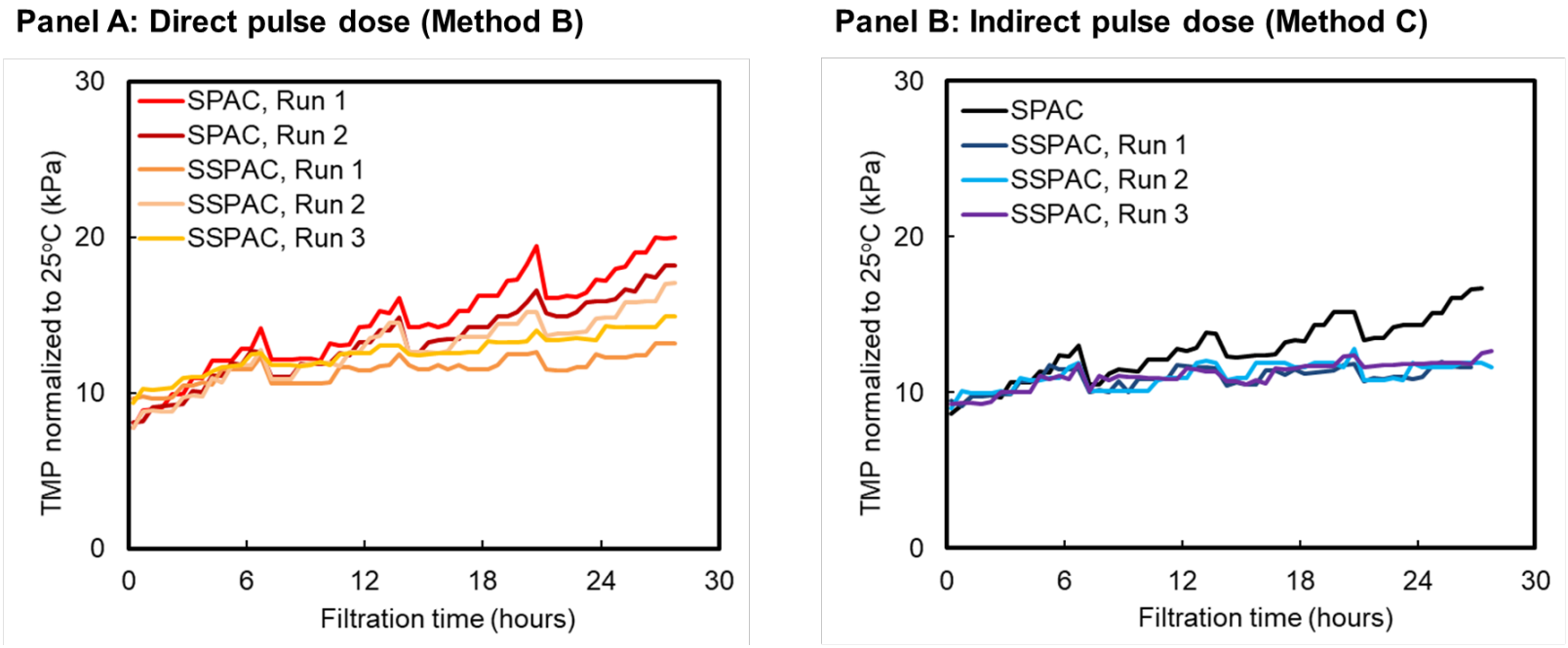

Fig. 18S —TMP versus filtration time when membrane filtration was conducted after SPAC/SSPAC adsorption and coagulation pretreatment. Direct (Panel A) and indirect (Panel B) pulse dose (explained in Figs. 3S, 4S, and 7S, SI) were used in this experiment. Backwash interval was 7 hours. Filtration rate was 1.7 m/day (70.8 L/m^{2}h). Raw water-2 was used in this experiment.